Possible Involvement of CD81 in Acrosome Reaction of Sperm in Mice

MAYA TANIGAWA,[1,2] KIYOKO MIYAMOTO,[1] SATOSHI KOBAYASHI,[3] MASAHIRO SATO,[4] HIDENORI AKUTSU,[1] MASARU OKABE,[2,5] EISUKE MEKADA,[3] KEIICHI SAKAKIBARA,[1] MAMI MIYADO,[1] AKIHIRO UMEZAWA,[1] AND KENJI MIYADO[1,6,7]*

[1]*Department of Reproductive Biology and Pathology, National Center for Child Health and Development, Tokyo, Japan*
[2]*Faculty of Pharmaceutical Sciences, Osaka University, Osaka, Japan*
[3]*Research Institute for Microbial Diseases, Osaka University, Osaka, Japan*
[4]*Frontier Science Research Center, Kagoshima University, Kagoshima, Japan*
[5]*Genome Information Research Center, Osaka University, Osaka, Japan*
[6]*PREST, Japan Science and Technology Agency, Saitama, Japan*
[7]*School of Biomedical Science, Tokyo Medical and Dental University, Tokyo, Japan*

ABSTRACT Tetraspanin CD81 is closely homologous in amino acid sequence with CD9. CD9 is well known to be involved in sperm–egg fusion, and CD81 has also been reported to be involved in membrane fusion events. However, the function of CD81 as well as that of CD9 in membrane fusion remains unclear. Here, we report that disruption of the mouse CD81 gene led to a reduction in the fecundity of female mice, and CD81−/− eggs had impaired ability to fuse with sperm. Furthermore, we demonstrated that when CD81−/− eggs were incubated with sperm, some of the sperm that penetrated into the perivitelline space of CD81−/− eggs had not yet undergone the acrosome reaction, indicating that the impaired fusibility of CD81−/− eggs may be in part caused by failure of the acrosome reaction of sperm. In addition, we showed that CD81 was highly expressed in granulosa cells, somatic cells that surround oocytes. Our observations suggest that there is an interaction between sperm and CD81 on somatic cells surrounding eggs before the direct interaction of sperm and eggs. Our results may provide new clues for clarifying the cellular mechanism of the acrosome reaction, which is required for sperm–egg fusion. *Mol. Reprod. Dev. 75: 150–155, 2008.* © 2007 Wiley-Liss, Inc.

Key Words: CD9; acrosome reaction; fertilization; mice; zona pellucida

INTRODUCTION

Fertilization is accomplished by the direct interaction of sperm and eggs, a process mediated primarily by predicted, but yet unidentified gamete membrane proteins. In fertilization, the acrosome reaction is a change in sperm that is required for penetration into the zona pellucida, the egg coat, and facilitates the subsequent fusion with the egg plasma membrane (Moreno and Alvarado, 2006). Zona pellucida protein 3 (ZP3), one of the components forming the meshwork of the zona pellucida, has been considered to be the prime physiological inducer of the acrosome reaction in sperm, although the frequency of acrosome reaction is low after incubation with recombinant ZP3 (Beebe et al., 1992). This discrepancy suggests that, besides ZP3, unknown major factor(s) might be responsible for the acrosome reaction. To date, despite the importance of the acrosome reaction in fertilization, the underlying cellular mechanisms that regulate the acrosome reaction remain unclear.

Two tetraspanins, CD9 and CD81, are known to be important in the membrane fusion events in various biological systems. In virus-host cell fusion, human CD81 has been identified as a co-receptor for hepatitis C virus (Higginbottom et al., 2000; Cormier et al., 2004). Both CD9 and CD81 have been implicated in myoblast fusion (Tachibana and Hemler, 1999; Schwander et al., 2003) and monocyte/macrophage fusion in mice (Takeda et al., 2003). Recent studies using gene-targeting techniques demonstrated that female mice carrying a deletion of the CD9 gene produce eggs that mature normally but are defective in sperm–egg fusion (Kaji et al., 2000; Le Naour et al., 2000; Miyado et al., 2000; Takahashi et al., 2001). CD81 has also been reported to be expressed on the plasma membrane of unfertilized mouse eggs (Takahashi et al., 2001). Furthermore, CD81−/− mice have been reported to have defects in reproduction after several generations of backcrossing (Deng et al., 2000).

Grant sponsor: Precursory Research for Embryonic Science and Technology (PRESTO); Grant sponsor: The Ministry of Health, Labour and Welfare; Grant sponsor: The Ministry of Education, Culture, Sports, and Technology, of Japan.

*Correspondence to: Kenji Miyado, National Center for Child Health and Development, 2-10-1 Okura, Setagaya, Tokyo 157-8535, Japan. E-mail: kmiyado@nch.go.jp

Received 31 October 2006; Accepted 8 December 2006
Published online 8 February 2007 in Wiley InterScience (www.interscience.wiley.com).
DOI 10.1002/mrd.20709

Recently, Rubinstein et al. (2006) provided more detailed data showing that eggs of CD81−/− mice are unable to be fertilized with sperm, although the degree of the defect appeared not to be severe compared with that of CD9−/− eggs. Moreover, injection of CD9−/− eggs with mouse CD81 mRNA revealed that mouse CD81 was only moderately effective at reversing the infertility of CD9−/− eggs (Kaji et al., 2002). These findings taken together indicate that CD81 and CD9 each have different roles in fertilization.

Here we studied the role of CD81 in fertilization by in vitro fertilization (IVF) and immunohistochemical analysis, and propose a possible role of CD81 in the acrosome reaction in sperm.

MATERIALS AND METHODS

Animals

CD81−/− mice (Miyazaki et al., 1997) were kindly provided by Dr. Miyazaki and were backcrossed to C57BL/6 mice. Genotyping was carried out using polymerase chain reaction as previously described (Miyazaki et al., 1997). To visualize acrosome-intact sperm, EGFP-transgenic mice expressing EGFP in the acrosomes were generated by pronuclear injection of constructs carrying the EGFP gene driven by the mouse acrosin promoter (Nakanishi et al., 1999) and the DsRed2 gene tagged with a mitochondrial transport signal and driven by the CAG promoter into fertilized eggs of BDF1 mice (unpublished information). After the sperm were acrosome-reacted, EGFP was lost from the sperm heads and DsRed remained in the mitochondria of the mid-piece region. All animal procedures were performed according to protocols approved by the National Center for Child Health and Development and use committees.

Egg Collection

Female mice (aged 8–15 weeks) were injected with 5 U of hCG (Gonatropin; Aska Pharmaceutical Co., Ltd, Tokyo, Japan) 48 hr after administration of 5 U of PMSG (Serotropin; Aska Pharmaceutical Co., Ltd). Ovulated eggs were collected from the oviductal ampulla 13.5–15 hr after hCG injection, and placed in 100-μl drops of TYH medium equilibrated with 5% CO_2 in air at 37°C. Cumulus cells were removed with 300 IU/ml of hyaluronidase (H-3506, Sigma-Aldrich, Missouri, MO), and eggs were incubated with a defined number of sperm.

Sperm Preparation and In Vitro Fertilization

Sperm were collected by squeezing two cauda epididymides of 8- to 10-week-old B6C3F1 or transgenic male mice in a well containing 100-μl of TYH medium. Sperm were incubated at 37°C in 5% CO_2 for 90 min before being mixed with eggs derived from wild-type or CD81−/− female mice. The final concentration of sperm added to an egg-containing drop was 1.5×10^5 sperm/ml. To examine the rate of fertilization, we counted the number of eggs at the two-cell stage 24 hr after incubation with the sperm. For counting the number of fused sperm, the zona pellucida was removed from the eggs by a brief incubation in acid Tyrode solution, and sperm were incubated with eggs preloaded with 4′,6-diamidino-2-phenylindole (DAPI) for counting the number of sperm fused with eggs (Yamagata et al., 2002). For counting the number of acrosome-intact sperm, EGFP-expressing sperm were incubated with zona-intact CD81+/+ or CD81−/− eggs. The eggs were all subjected to confocal microscopic analysis for the presence of sperm exhibiting red and green fluorescence or red fluorescence alone within the perivitelline space 4 hr after incubation.

Immunostaining

For immunostaining of cryostat sections, ovaries from 8- to 10-week-old wild-type C57BL/6 females were fixed in 2% paraformaldehyde in PBS (−) for 2 days at 4°C, and then immersed in 30% sucrose in PBS (−) for more than 2 days at 4°C, embedded in Tissue-Tek OCT compound (Sakura Finetek Co., Tokyo, Japan), and finally frozen before serial cryostat sectioning (8 μm in thickness). Slides were fixed in an acetone and incubated with anti-CD81 antibody (Eat-1) diluted 1:300 in PBS (−) containing 0.1% bovine serum albumin (BSA), BSA/PBS (−), or anti-ZP3 antibody diluted 1:300 in BSA/PBS (−), overnight at 4°C. After washing three times with BSA/PBS (−), the samples were incubated with Alexa 546-conjugated goat anti-hamster IgG (A-21111, Invitrogen, California, CA) or Alexa 488-conjugated goat anti-rat IgG (A-11006, Invitrogen) for 2 hr at room temperature. After extensive washing, the slides were inspected for fluorescence using LSM 510 META confocal microscope.

Immunoblotting

Samples containing equal amounts of eggs were dissolved in nonreducing sample buffer and subjected to 12% SDS–PAGE according to procedures described previously (Miyado et al., 2000). After electrophoresis, the gels were transferred to PVDF membranes for immunoblot analysis. The blots were blocked in 1% nonfat dry milk, and were probed with the primary antibodies, anti-mouse CD81 antibody (Eat-1, BD Biosciences, California, CA) or anti-mouse CD9 antibody (KMC8, BD Biosciences). After washing in TBS-Tween buffer, the membranes were incubated with HRP-labeled secondary antibodies; goat anti-rat antibody or goat anti-hamster antibody. The expression level of immunoreacted products was determined by treatment of the blots with an ECL or ECL Plus Detection Kit (GE Healthcare Bio-Science Co., New Jersey, UK) and exposure to X-ray film at room temperature.

Statistical Analysis

Data from different groups were tested by the *t*-test for the significance of the difference between the means of two independent samples using the computer software KaleidaGraph (version 3.6, Synergy Software, Inc., Pennsylvania, PA).

RESULTS

Female Fertility Impaired by CD81 Deficiency

Figure 1A depicts the average litter size in matings of three genotypes of females, wild-type, CD81+/− and CD81−/− mice, with CD81+/− males over a period of 6 months. Although these females displayed normal mating behavior with the males (data not shown), the average litter size of CD81−/− females was markedly reduced relative to those of CD81+/− and wild-type mice (on average, 1.3 ± 2.5 vs. 11.3 ± 1.3 and 11.0 ± 0.8) (Fig. 1A). To examine the oocyte maturation and ovulation, we also collected the eggs from mice superovulated by stimulation with exogenous gonadotropin. The eggs collected from CD81−/− mice were indistinguishable with regard to morphology and number (on average, 18.0 ± 2.8) from those wild-type and CD81+/− mice (on average, 19.9 ± 1.7 and 21.7 ± 2.8) (Fig. 1B). Therefore, the reduction in fertility of CD81−/− females did not seem to be due to defects of ovulation or oocyte maturation.

Involvement of CD81 in Fertilization

To clarify the cause of the reduced fertility of CD81−/− females, the function of CD81−/− eggs was further examined by IVF. When cumulus oocyte complexes (COCs) collected from CD81−/− or wild-type control mice were incubated with the wild-type sperm, the sperm could disperse cumulus cells, somatic cells surrounding eggs, and reach and apparently penetrate the zona pellucida of CD81−/− and wild-type eggs. However, the average rate of eggs developing to the two-cell stage was substantially decreased for CD81−/− eggs (on average, $15.0 \pm 2.5\%$) compared with that for wild-type eggs (on average, $65.0 \pm 10.8\%$) 24 hr after incubation with the sperm (Fig. 1D). Furthermore, in CD81−/− eggs, several sperm were observed in the perivitelline space (Fig. 1C). The delayed formation of two-cell embryos and the accumulation of more than one sperm within the perivitelline space in CD81−/− eggs demonstrate that CD81−/− eggs have impaired ability of fertilization. Subsequently, to examine the cause of the impaired fertilization, we performed IVF for CD81−/− eggs and wild-type eggs after the zona pellucida was removed using acid Tyrode solution (Fig. 2A,B). To measure the number of sperm fused with eggs, both types of eggs were preloaded with DAPI before incubation with wild-type sperm (Yamagata et al., 2002). One hour after insemination, estimation of the average number of sperm fused with one egg by measurement of DAPI fluorescence revealed that CD81−/− eggs showed a decreased number of fused sperm (on average, 1.21 ± 0.23) in comparison with the wild-type eggs (on average, 1.95 ± 0.27). Those results suggest that CD81 is involved in sperm–egg fusion, either directly or indirectly.

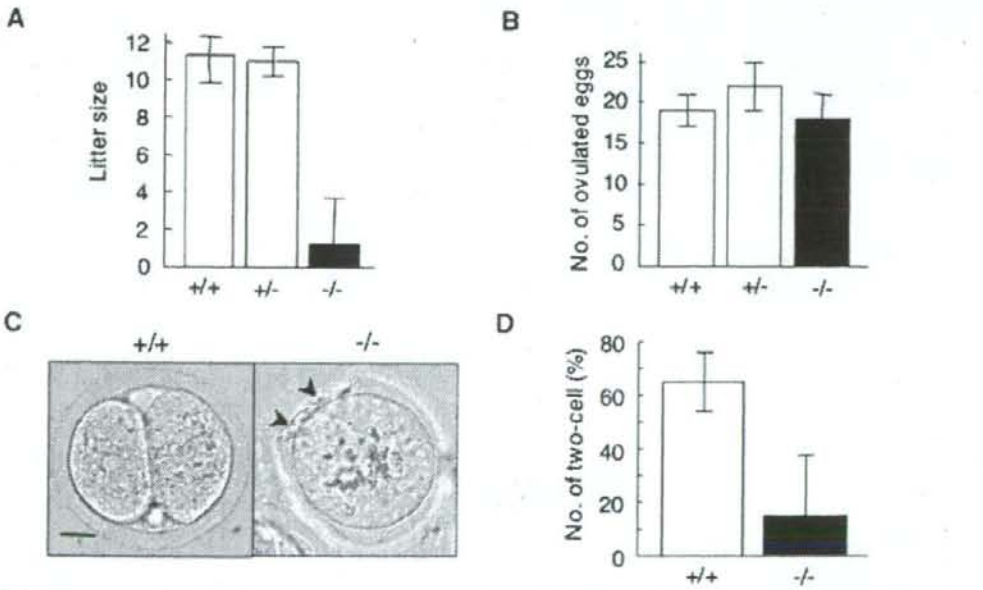

Fig. 1. Female infertility caused by CD81 deficiency. **A**: Average litter sizes of crosses between CD81+/− males and three types of females, wild-type, CD81+/− and CD81−/− mice. Each of the mating pairs was kept in a separate cage, and births over a 6-month period were monitored. Data of births during successive 2-month periods were grouped together, and the average litter size of wild-type, CD81+/− and CD81−/− females was calculated from data recorded for five mating pairs 8–15 weeks of age at the start of the experiment. **B**: Average number of ovulated eggs from wild-type, CD81+/− and CD81−/− female mice. The eggs were collected 13.5–16 hr after hCG treatment, and counted. **C**: Representative micrographs of CD81+/+ and CD81−/− eggs. The eggs were obtained 24 hr after incubation with the wild-type sperm. **D**: Average number of eggs that developed to the two-cell stage 24 hr after incubation with the wild-type sperm. The black bars show the results for CD81−/− eggs (A,B,D). Error bars represent SEM (A,B,D). Scale bar, 20 μm (C).

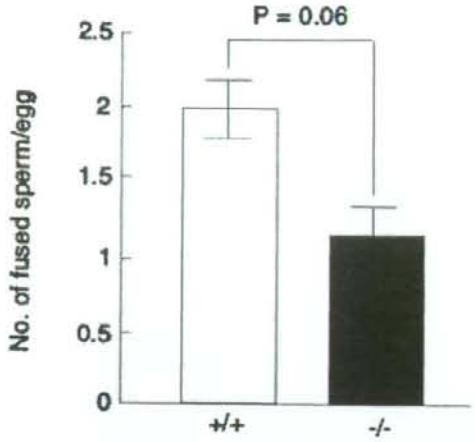

Fig. 2. In vitro sperm–egg fusion. Average number of sperm fused with wild-type or CD81−/− eggs after 3 hr of incubation. Error bars represent SEM. Data from different groups were tested by the *t*-test for the significance of the difference between the means of two independent samples ($P = 0.06$).

Expression of CD9 in CD81−/− Eggs

The mechanisms by which CD81 acts are still unclear. However, CD81 tends to form multimolecular complexes in which tetraspanins associate with specific proteins depending on the type of cell. In B cells, CD81 directly associates with CD19, taking part in the CD19-CD21-CD81 signaling complex (Pileri et al., 1998), which accords with the evidence that the expression of CD19 in bone marrow, spleen, and peripheral B cells is reduced in CD81−/− mice (Miyazaki et al., 1997). As previously mentioned, CD9 on the egg plasma membrane is required for fusion with sperm, and the impaired fusibility of CD81−/− eggs with sperm may likely be dependent on the expression of CD9. To investigate whether CD81 deficiency may cause downregulation of CD9 expression, the expression level of CD9 was examined (Fig. 3). We collected three types of eggs, wild-type, CD81+/− and CD81−/− eggs, 13.5–15 hr after hCG injection into mice, and examined the expression level of CD9 in comparison with that of CD81 by SDS–PAGE. The amounts of CD81 were invariable in wild-type and CD81+/− eggs, but CD81 was lost in CD81−/− eggs. By contrast, there were no significant differences in the expression of CD9 among these eggs. Therefore, the impairment of fertilization caused by CD81 deficiency cannot be attributed to decreased expression of CD9 in eggs.

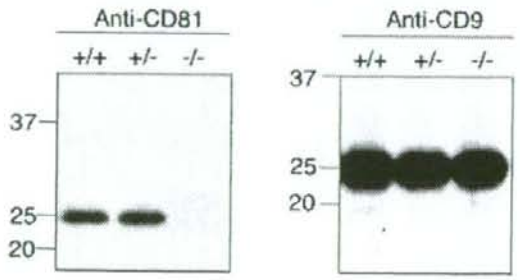

Fig. 3. The expression of CD9 in wild-type, CD81+/− and CD81−/− eggs. Proteins were isolated from the types of eggs indicated and resolved by sodium dodecyl sulfate polyacrylamide gel electrophoresis under nonreducing conditions. The proteins were electrophoretically transferred to a membrane, where they were probed with antibodies to CD81 (**panel A**) and CD9 (**panel B**). The proteins corresponding to each 110 egg (panel A) and 10 eggs (panel B) were analyzed.

Expression of CD81 During Folliculogenesis

The expression and localization of CD81 in ovarian tissues were immunohistochemically assessed using cryostat sections of adult wild-type ovaries. The follicles consist of immature eggs and granulosa cells that surround the egg; a single follicle usually grows to the preovulatory stage and releases the egg for potential fertilization (Buccione et al., 1990). Immunohistochemical staining with anti-CD81 mAb demonstrated that CD81 was continuously expressed in the egg and surrounding follicles (Fig. 4), and in cumulus cells surrounding ovulated eggs (data not shown). These data indicate that the sperm may encounter CD81 on the somatic cells surrounding eggs before direct interaction of sperm and eggs.

Possible Involvement of CD81 in Acrosome Reaction

Based on the localization of CD81 and the impaired fertilization of CD81−/− eggs, we speculated that the inability of wild-type sperm to fuse CD81−/− eggs might be due to impairment of prefusional stages, including the acrosome reaction. To examine the involvement of CD81 in the acrosome reaction of the sperm, CD81−/− eggs or wild-type eggs were incubated with the sperm collected from transgenic mice specifically expressing enhanced green fluorescent protein (EGFP) in the acrosomes (Fig. 5). The acrosome corresponds functionally to a lysosome and thus contains lysosomal enzymes (Moreno and Alvarado, 2006), and acrosin is a sperm acrosomal serine proteinase that is lost from the sperm head after the acrosome reaction is completed (Baba et al., 1994). Therefore, sperm expressing EGFP at the acrosomes in the heads are useful for the detection of acrosome-intact sperm. After 3 hr of incubation, we counted the number of acrosome-intact sperm within the perivitelline spaces. To count the sperm that had penetrated into the zona pellucida, the eggs were incubated with 3.0×10^5 sperm/ml. When the number of sperm within the perivitelline space were counted 3 hr after incubation with the eggs, we observed that an increased percentage ($8.5 \pm 2.3\%$) of the sperm that had penetrated into the perivitelline space of CD81−/− eggs exhibited EGFP fluorescence in their head portion. In contrast, very few sperm that had penetrated into the perivitelline space of wild-type eggs exhibited green fluorescence ($1.4 \pm 1.0\%$). These results suggest that the sperm that penetrated into the zona pellucida of the CD81−/− eggs were impaired in the acrosome reaction.

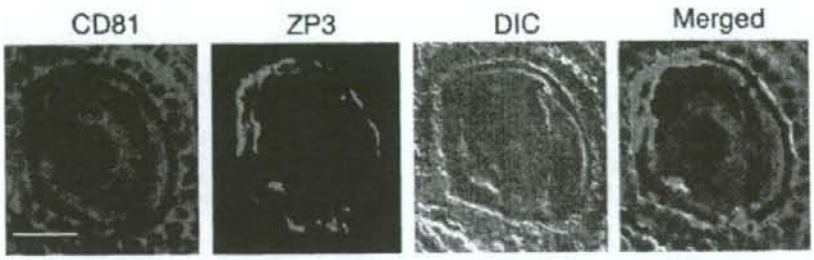

Fig. 4. CD81 is expressed at high levels in granulosa cells during oogenesis. Frozen sections of ovaries from wild-type mice were stained with anti-mouse CD81 mAb and with anti-ZP3 mAb. DIC represents a photograph taken by differential interference contrast. Scale bar, 20 μm. [See color version online at www.interscience.wiley.com.]

DISCUSSION

CD81 has been suggested to be a protein playing a role in membrane fusion events, but the function of CD81 in sperm–egg fusion remains unknown. As suggested by Rubinstein et al. (2006), CD9 and CD81 may have different roles in sperm–egg fusion. This notion is supported by the following facts: (1) deletion of a single gene, CD9 or CD81, causes impaired fertilization, and the expression of CD9 on eggs is not perturbed by CD81 deficiency, and (2) CD9−/− eggs injected with mRNA encoding CD81 cannot be fully rescued to the same degree as those injected with CD9 mRNA (Kaji et al., 2002).

Generally, the acrosome reaction is a change in the membrane of sperm that are activated for penetration into zona pellucida and facilitates the subsequent fusion with the egg membrane (Baba et al., 1994). During the acrosome reaction, the disruption of the acrosome covering the sperm head causes the release of acrosin and other proteolytic substances. As previously reported (Moreno and Alvarado, 2006), these materials included in the acrosome are important for the penetration of sperm into the zona pellucida and for sperm–egg fusion, but the molecular mechanism underlying the acrosome reaction is largely unknown. When wild-type eggs were incubated with sperm expressing EGFP in the acrosomes, we found the presence of acrosome-intact

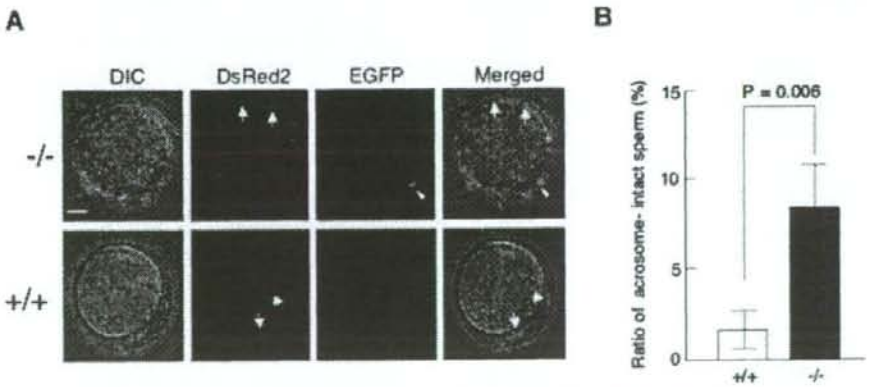

Fig. 5. In vitro fertilization assay for acrosome reaction. **A**: Representative photographs. CD81−/− eggs were incubated with transgenic sperm expressing EGFP at acrosomes in the sperm heads. Eggs from wild-type females were also subjected to fertilization using the AR-GFP transgenic sperm as controls. Four hours after insemination, the eggs were inspected for fluorescence using a confocal microscope. As shown in the **upper panel**, some CD81−/− eggs had sperm with green fluorescence (indicated by arrowheads) in their head region in the perivitelline space, while almost no wild-type eggs had such types of sperm (**lower panel**). Photomicrographs taken under light (DIC); photomicrographs taken for detecting DsRed2 translocated to mitochondria by the retention signal (Mt-DsRed2) and specifically expressed in the mid-piece of sperm (indicated by arrows); photomicrographs taken for detecting EGFP-derived green fluorescence specifically expressed in the head region of sperm (indicated by arrowheads); merged images. Scale bar, 20 μm. **B**: Examination of acrosome reaction using EGFP-expressing sperm. CD81−/− or wild-type eggs were fertilized in vitro with epididymal sperm expressing EGFP in the acrosomes. Four hours after insemination, the sperm entering into the perivitelline space were inspected for fluorescence using a confocal microscope. Note that the number of sperm carrying intact acrosomes (exhibiting green fluorescence in the sperm head region, as shown in A) and entering into the perivitelline space of CD81−/− eggs was significantly higher than that of acrosome-intact sperm entering into the perivitelline space of wild-type eggs. Acrosome-intact sperm can easily be detected since they exhibit bright green fluorescence in their head region. The total number of sperm entered into perivitelline space can be counted by inspection for red fluorescence in the mid-piece of the sperm. [See color version online at www.interscience.wiley.com.]

sperm in the outer layer of the zona pellucida (data not shown), but almost all sperm that penetrated into the perivitelline space had lost the acrosome caps (Fig. 5). These findings suggest that the acrosome reaction may occur in the perivitelline space and/or inner layer of the zona pellucida.

Another possible reason for the failure of the acrosome reaction of EGFP-expressing sperm in CD81−/− eggs is that "zona hardening" in CD81−/− eggs may not be sufficient compared to that in wild-type eggs. The weakened zona hardening might permit the penetration of some acrosome-intact sperm into CD81−/− eggs. However, since proteins other than components forming the zona pellucida may be triggers for preventing polyspermy and zona hardening (Sun, 2003), it would be of interest to test whether CD81 and ZP3 interact with each other.

In conclusion, the results of our IVF experiments suggest the possible involvement of CD81 in the acrosome reaction of zona pellucida-penetrated sperm prior to the fusion of sperm with eggs. Extensive attempts to elucidate the role of CD81 in the acrosome reaction are now underway.

ACKNOWLEDGMENTS

We are thankful for Dr. Tsujimoto (Faculty of Medicine, Osaka University) for kindly providing mt-DsRed2 contract for transgenic production. This work was supported by a grant from Precursory Research for Embryonic Science and Technology (PRESTO), The Ministry of Health, Labour and Welfare, and a grant-in aid for Scientific Research, The Ministry of Education, Culture, Sports, and Technology, of Japan.

REFERENCES

Baba T, Azuma S, Kashiwabara S, Toyoda Y. 1994. Sperm from mice carrying a targeted mutation of the acrosin gene can penetrate the oocyte zona pellucida and effect fertilization. J Biol Chem 269: 31845–31849.

Beebe SJ, Leyton L, Burks D, Ishikawa M, Fuerst T, Dean J, Saling P. 1992. Recombinant mouse ZP3 inhibits sperm binding and induces the acrosome reaction. Dev Biol 151:48–54.

Buccione R, Schroeder AC, Eppig JJ. 1990. Interactions between somatic cells and germ cells throughout mammalian oogenesis. Biol Reprod 43:543–547.

Cormier EG, Tsamis F, Kajumo F, Durso RJ, Gardner JP, Dragic T. 2004. CD81 is an entry coreceptor for hepatitis C virus. Proc Natl Acad Sci USA 101:7270–7274.

Deng J, Yeung VP, Tsitoura D, DeKruyff RH, Umetsu DT, Levy S. 2000. Allergen-induced airway hyperreactivity is diminished in CD81-deficient mice. J Immunol 165:5054–5061.

Higginbottom A, Quinn ER, Kuo CC, Flint M, Wilson LH, Bianchi E, Nicosia A, Monk PN, McKeating JA, Levy S. 2000. Identification of amino acid residues in CD81 critical for interaction with hepatitis C virus envelope glycoprotein E2. J Virol 74:3642–3649.

Kaji K, Oda S, Miyazaki S, Kudo A. 2002. Infertility of CD9-deficient mouse eggs is reversed by mouse CD9, human CD9, or mouse CD81; polyadenylated mRNA injection developed for molecular analysis of sperm-egg fusion. Dev Biol 247:327–334.

Kaji K, Oda S, Shikano T, Ohnuki T, Uematsu Y, Sakagami J, Tada N, Miyazaki S, Kudo A. 2000. The gamete fusion process is defective in eggs of Cd9-deficient mice. Nat Genet 24:279–282.

Le Naour F, Rubinstein E, Jasmin C, Prenant M, Boucheix C. 2000. Severely reduced female fertility in CD9-deficient mice. Science 287:319–321.

Miyado K, Yamada G, Yamada S, Hasuwa H, Nakamura Y, Ryu F, Suzuki K, Kosai K, Inoue K, Ogura A, Okabe M, Mekada E. 2000. Requirement of CD9 on the egg plasma membrane for fertilization. Science 287:321–324.

Miyazaki T, Muller U, Campbell KS. 1997. Normal development but differentially altered proliferative responses of lymphocytes in mice lacking CD81. EMBO J 16:4217–4225.

Moreno RD, Alvarado CP. 2006. The mammalian acrosome as a secretory lysosome: New and old evidence. Mol Reprod Dev 73:1430–1434.

Nakanishi T, Ikawa M, Yamada S, Parvinen M, Baba T, Nishimune Y, Okabe M. 1999. Real-time observation of acrosomal dispersal from mouse sperm using GFP as a marker protein. FEBS Lett 449:277–283.

Pileri P, Uematsu Y, Campagnoli S, Galli G, Falugi F, Petracca R, Weiner AJ, Houghton M, Rosa D, Grandi G, Abrignani S. 1998. Binding of hepatitis C virus to CD81. Science 282:938–941.

Rubinstein E, Ziyyat A, Prenant M, Wrobel E, Wolf JP, Levy S, Le Naour F, Boucheix C. 2006. Reduced fertility of female mice lacking CD81. Dev Biol 290:351–358.

Schwander M, Leu M, Stumm M, Dorchies OM, Ruegg UT, Schittny J, Muller U. 2003. Beta1 integrins regulate myoblast fusion and sarcomere assembly. Dev Cell 4:673–685.

Sun QY. 2003. Cellular and molecular mechanisms leading to cortical reaction and polyspermy block in mammalian eggs. Microsc Res Tech 61:342–348.

Tachibana I, Hemler ME. 1999. Role of transmembrane 4 superfamily (TM4SF) proteins CD9 and CD81 in muscle cell fusion and myotube maintenance. J Cell Biol 146:893–904.

Takahashi Y, Bigler D, Ito Y, White JM. 2001. Sequence-specific interaction between the disintegrin domain of mouse ADAM 3 and murine eggs: Role of beta1 integrin-associated proteins CD9, CD81, and CD98. Mol Biol Cell 12:809–820.

Takeda Y, Tachibana I, Miyado K, Kobayashi M, Miyazaki T, Funakoshi T, Kimura H, Yamane H, Saito Y, Goto H, Yoneda T, Yoshida M, Kumagai T, Osaki T, Hayashi S, Kawase I, Mekada E. 2003. Tetraspanins CD9 and CD81 function to prevent the fusion of mononuclear phagocytes. J Cell Biol 161:945–956.

Yamagata K, Nakanishi T, Ikawa M, Yamaguchi R, Moss SB, Okabe M. 2002. Sperm from the calmegin-deficient mouse have normal abilities for binding and fusion to the egg plasma membrane. Dev Biol 250:348–357.

REPRODUCTION
REVIEW

What can we learn from gene expression profiling of mouse oocytes?

Toshio Hamatani[1,2], Mitsutoshi Yamada[1,2], Hidenori Akutsu[2], Naoaki Kuji[1], Yoshiyuki Mochimaru[1], Mitsuko Takano[1], Masashi Toyoda[2], Kenji Miyado[2], Akihiro Umezawa[2] and Yasunori Yoshimura[1]

[1]*Department of Obstetrics and Gynecology, Keio University School of Medicine, 35 Shinanomachi Shijuku-ku, Tokyo 160-8582, Japan and* [2]*Department of Reproductive Biology and Pathology, National Institute for Child Health and Development, 2-10-1 Okura Setagaya-ku, Tokyo 157-8535, Japan*

Correspondence should be addressed to T Hamatani; Email: t-hama@sc.itc.keio.ac.jp

Abstract

Mammalian ooplasm supports the preimplantation development and reprograms the introduced nucleus transferred from a somatic cell to confer pluripotency in a cloning experiment. However, the underlying molecular mechanisms of oocyte competence remain unknown. Recent advances in microarray technologies have allowed gene expression profiling of such tiny specimens as oocytes and preimplantation embryos, generating a flood of information about gene expressions. So, what can we learn from it? Here, we review the initiative global gene expression studies of mouse and/or human oocytes, focusing on the lists of maternal transcripts and their expression patterns during oogenesis and preimplantation development. Especially, the genes expressed exclusively in oocytes should contribute to the uniqueness of oocyte competence, driving mammalian development systems of oocytes and preimplantation embryos. Furthermore, we discuss future directions for oocyte gene expression profiling, including discovering biomarkers of oocyte quality and exploiting the microarray data for 'making oocytes'.

Reproduction (2008) **135** 581–592

Introduction

The mammalian oocyte is marked by extraordinary biological competence; it can haploidize its DNA, be fertilized and reprogram the sperm chromatin into a functional pronucleus, induce zygotic genome activation (ZGA), give rise to totipotency, and drive early embryonic development. Using its ability to reprogram a somatic nucleus transferred into an enucleated oocyte, derivation of embryonic stem (ES) cells from cloned blastocysts for therapeutic cloning is explored. The molecular mechanisms underlining such oocyte competence are largely unknown.

On the other hand, the reproductive capacity of women declines dramatically beyond the mid-30s (van Kooij *et al.* 1996, ASRM/SART 2000, Armstrong 2001, Klein & Sauer 2001), which is mainly caused by age-related decline in oocyte quality. For example, young women undergoing standard *in vitro* fertilization (IVF) with their own eggs show a success rate comparable with older women (>40 years) undergoing IVF with eggs donated by this younger subset of women (Navot *et al.* 1991). To overcome age-related decline in oocyte quality, ooplasmic donation has been performed by injecting ooplasm from a young, healthy donor oocyte into a patient oocyte to improve the outcome of assisted reproduction techniques (Cohen *et al.* 1997, 1998, Takeuchi *et al.* 1999). There is, however, little molecular evidence supporting the efficacy and the safety of ooplasmic donation. Furthermore, no molecular biomarker for oocyte quality has been established. Oocyte quality based on a morphological grading system is the only reliable prognostic factor in human IVF programs. Studies of molecular mechanisms involved in oocyte quality could have important implications for the efficacy and safety of clinical ooplasmic donation.

Thus, understanding the molecular mechanisms in oocytes is quite important for both reproductive biology and regenerative medicine. The scarcity of the materials, however, both in size (diameter <100 um) and in quantity (only a few to tens of oocytes from each ovulation in mice), has hampered the molecular analysis of oocytes. Earlier attempts to analyze oocytes employed RT-PCR and differential display using only a few candidate genes. In addition, serial analysis of gene expression (SAGE) and cDNA libraries were generated from mouse and human oocytes, and SAGE tags and expressed sequence tags (ESTs) were sequenced for rapid gene discovery and expression profiling in oocytes

ISSN 1470-1626 (paper) 1741-7899 (online)
DOI: 10.1530/REP-07-0430
Online version via www.reproduction-online.org

(Ko *et al.* 2000, Ko 2004, Adjaye 2005, Evsikov *et al.* 2006). Furthermore, the recent progress in RNA amplification methods and microarray platforms including genes unique to oocytes and preimplantation embryos allows us to apply global gene expression profiling to the studies of the oocytes and preimplantation embryos (Carter *et al.* 2003). To date, several reports of the oocyte transcriptome using unique biological models have been published (Dobson *et al.* 2004, Hamatani *et al.* 2004*a*, 2004*b*, Wang *et al.* 2004, Zeng *et al.* 2004, Pan *et al.* 2005, Assou *et al.* 2006, Kocabas *et al.* 2006, Yoon *et al.* 2006). The identification of a large number of genes expressed in oocytes, especially oocyte-specific genes, and multiple signaling pathways in the models by such global gene expression profiling is the first step toward understanding oocyte quality and the molecular mechanisms underlying oogenesis, developmental programs, and totipotency in preimplantation embryos.

Global gene expression profiling of mouse preimplantation embryos to dissect maternal transcripts

Two groups simultaneously published the first reports on global gene expression profiling of all stages of preimplantation embryos (Fig. 1; Hamatani *et al.* 2004*a*, Wang *et al.* 2004). While Wang *et al.* used the Affymetrix 25-mer oligo DNA microarray system, we used the NIA 60-mer oligo microarray (Agilent Mouse Development Array), which is enriched for genes expressed in stem cells and preimplantation embryos (Carter *et al.* 2003). Taking advantage of 60-mer oligo DNA hybridization kinetics (Hughes *et al.* 2001), it was also optimized for use with tiny amounts of RNA (Carter *et al.* 2003). During preimplantation development, 12 179 out of 21 939 gene features on the NIA 60-mer oligo microarray showed statistically significant changes with false discovery rate (FDR) $<10\%$ by ANOVA-FDR test. Pair-wise comparison, hierarchical clustering analysis, and principal component analysis (PCA) revealed two major transient waves of *de novo* transcription (Fig. 1A–C). The first wave corresponds to ZGA. The second wave, mid-preimplantation gene activation (MGA), contributes to dramatic morphological changes during late preimplantation development.

To trace the expression changes of individual genes, 12 179 statistically significant genes were analyzed by *k*-means clustering method and 9 clusters were identified (Fig. 2). Gene expression patterns of these clusters can be assigned to three main groups. The first group appears to represent ZGA genes that are first activated from the zygotic genome (Clusters 1, 4, 5, and 8). The list of the ZGA genes suggests that ZGA is not promiscuous as previously proposed and contributes mainly to the preparation of basic cellular machinery during the two-cell and the four-cell stages.

The second group represents maternal transcripts with distinctive patterns of degradation during preimplantation development (Clusters 7 and 9). Although the massive maternal RNA degradation pattern by the two-cell stage is confirmed (Cluster 9) as previous studies suggested (Nothias *et al.* 1995, Schultz 2002), 70.5 and 32.5% of the transcripts in Clusters 7 and 9 respectively further show significant reduction from the four-cell to eight-cell stages. Selective degradation of maternal transcripts during oocyte maturation is, as also shown by the latest study (Su *et al.* 2007), a developmentally regulated event preceding the transition of gene expression from maternal to zygotic control. Since most genes in Clusters 7 and 9 are not reactivated during preimplantation development, the genes in these clusters are suggested to have specific functions either in oogenesis, oocyte maturation, fertilization, and/or early phases of preimplantation development.

The third group appears to represent genes that follow a combination of these two patterns (Clusters 2 and 3); 3329 genes whose expression first significantly increase from the four-cell to eight-cell stages are identified as the MGA genes, and 82.7 and 12.3% of them fall into Clusters 2 and 3 respectively. Further expression profiling of embryos treated with inhibitors of transcription and translation reveals that the translation of maternal RNAs is required for the initiation of ZGA, suggesting a cascade of gene activation from maternal RNA/protein sets to ZGA gene sets and thence to MGA gene sets (Hamatani *et al.* 2004*a*).

By MAPPFinder (Dahlquist *et al.* 2002, Doniger *et al.* 2003), which is a tool to identify global biological trends in gene expression data by interacting the annotations of Gene Ontology (GO) terms (Ashburner *et al.* 2000), the genes in the clusters of maternal transcripts are associated to such GO terms as 'circadian rhythm,' 'M-phase of mitotic cell cycle,' 'DNA replication,' 'Golgi apparatus/intracellular protein transport,' 'adherent junction,' 'small GTPase regulatory/interacting protein,' and 'intracellular signaling cascade'. The 'circadian rhythm' category includes seven mammal known circadian genes: *Per1–3*, *Cry1–2*, *Bmal1/Arntl*, and *Clock*. The transcripts of *Bmal1/Arntl*, *Clock*, *Timeless*, *Cry1*, and *Csnk1e* decrease during the one-cell to two-cell stages as previous reports showed (Johnson *et al.* 2002).

The egg–sperm fusion at fertilization in mammals releases an oocyte from metaphase II arrest by increasing Ca^{2+} levels, activating Ca^{2+}-calmodulin kinase II, and targeting cyclin B and c-mos for degradation via the ubiquitin–proteasome pathway. *Rfpl4*, an E3 ubiquitin protein ligase, regulates the degradation of cyclin B1 (*Ccnb1*) protein (Cluster 6b) (Suzumori *et al.* 2003), which is a well-known example of a transcript with a short poly(A) tail that is regulated at the post-transcriptional level in oocytes. Furthermore, *Cpeb*, *Eif4e*, *Cpsf2*, and *Stk13/Aurkc*, which are involved in the masking and/or translational regulation of transcripts with short

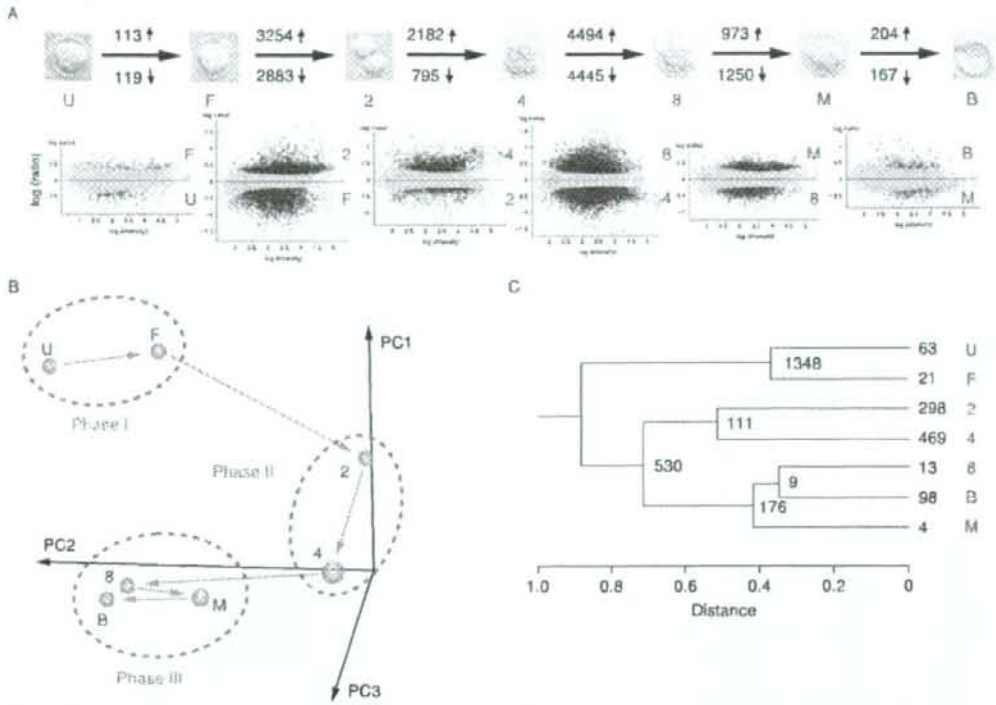

Figure 1 Global outlook of gene expression during preimplantation development (reprinted from 'Dynamics of global gene expression changes during mouse preimplantation development', Hamatani T *et al.* 2004 *Developmental Cell* **6** 117–131, with permission from Elsevier). (A) A matrix of scatter plots. U, F, 2, 4, 8, M, and B denote unfertilized egg, fertilized egg, two-cell embryo, four-cell embryo, eight-cell embryo, morula, and blastocyst respectively. Each scatter plot shows the comparison of gene expression between embryo stages. A horizontal axis represents the averaged log (intensity) of genes, whereas a vertical axis represents the log (ratio) of signal intensity for each gene between one stage and another stage. Colored spots (red and green) represent genes that passed the FDR = 10% statistical test. Red spots represent array features with higher expression at a later stage, whereas green spots represent array features with lower expression. (B) Principal component analysis. (C) Hierarchical clustering analysis. Numerical values represent the number of genes specific to each cluster or stage. A list of these stage-specific genes are available at the web site of Cell Press (Hamatani *et al.* 2004a).

poly(A) tails in oocytes (Hodgman *et al.* 2001, Mendez & Richter 2001), also decrease their transcripts by the two-cell stage. The presence of the 'DNA replication' category in oocytes indicates that oocytes are already well equipped with DNA replication machinery, as exemplified by the fact that neither the lack of *Zar1* (Wu *et al.* 2003) nor the presence of jasplakinolide, which is the most powerful known microfilament inhibitor (Terada *et al.* 2000), can prevent the initiation of DNA replication. In another global gene expression study of preimplantation embryos, DNA repair genes are also over-represented at the oocyte stage when compared with the one-cell through the blastocyst stages in their transcript profiling during preimplantation development (Zeng *et al.* 2004). Genes that are down-regulated from oocytes to two-cell embryos include many genes involved in DNA repairs, including *Orc1l*, *Orc4l*, *Orc5l*, *Orc6l*, *Mcm4*, *Pcna*, *Pola2*, *Polm*, *Blm*, *Top1*, and *Msh6* (Cluster 9); *Msh3* and *Mcm7* (Cluster 7); and *Cdc7l1/Cdc7*, *Cdc45l*, *Ccna2*, and *Dbf4/Ask* (Cluster 6). Furthermore, another group searched for maternal transcripts of polarity-regulating genes in mouse oocytes by global gene expression profiling of preimplantation embryos, which may subsequently control polarity in preimplantation embryos (Wang *et al.* 2004). They focused on three genes whose homologs have been shown to regulate cellular polarity in *Drosophila*: *Flamingo*, dystroglycan1 (*Dag1*), and cornichon (*Cnih2*) both of which are included by Cluster 3.

Global gene expression changes during oogenesis

Although several groups have studied global gene expression in human and mouse oocytes at the later stages of folliculogenesis (germinal vesicle stage and metaphase II stage; Wang *et al.* 2004, Cui *et al.* 2007,

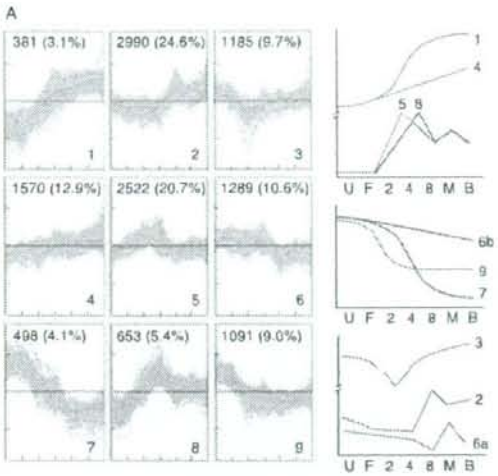

B

Cluster 6	Cluster 7	Cluster 9
Mater	*Gdf9*	*Mos/c-mos*
Ddx4/Vasa	*Obox1*	*Kit/c-kit*
Zp3	*Ezh2*	*Stat3*
Gata4	*Mad2l2*	*Cry1*
Frap1/mTOR	*Tcl1*	*Oosp1*
Fsrg1/Brd2	*Bmi1*	*Nobox/Og2x*
Baz1a	*Bmal1/Arntl*	*Cpeb1*
Cdc45l	*Clock*	*Magoh*
Ilk	*Zar1*	*Calna1*
Dtr/HB-EGF	*Rfpl4*	*N-cadherin*
Smarca5	*Mek1/Map2k1*	*Rac1*
Brd4	*Eps8*	*Hells/Lysh*
Son	*Stk13/AurkC*	*Mort4l2/MrgX*
Nfkbia/IkBa	*Ztp68*	*Baz1b*
Nfkb1/NF-kB	*Rnf35/2cz61*	*Zp1*
	Stmbt1	*Zp2*
	Spindlin	*Scml2*

Figure 2 Time-course analysis of individual genes. (Reprinted from 'Dynamics of global gene expression changes during mouse preimplantation development', Hamatani T *et al.* 2004 *Developmental Cell* **6** 117–131, with permission from Elsevier). (A) General trends of expression changes analyzed by *k*-means clustering method. The nine clusters were further classified into three super groups by visual inspection as shown in the three schemes in the far right column. (B) Representative genes in each cluster.

Gasca *et al.* 2007, Zhang *et al.* 2007), only two groups successfully performed global gene expression studies using mouse oocytes at the very early stages of folliculogenesis (Pan *et al.* 2005, Yoon *et al.* 2006). Pan *et al.* (2005) compared the transcriptomes of mouse oocytes obtained from day 2 primordial follicles to day 22 equine CG primed large antral follicles. From the primordial to large antral stages, 18 529 probe sets corresponding to 11 766 unigenes detected significant gene expression in oocytes that developed *in vivo*. The hierarchical clustering dendrogram and PCA analysis showed that the primordial oocyte is separated from oocytes obtained from the other stages. Many important genes encoding 'secreted proteins', which are defined on their own terms in that manuscript, display marked upregulation between the primordial and primary follicle stages (e.g., *Gdf9, Bmp15, Bmp5, Bmp6, Tgfb2, Tgfb3,* and several genes related to *Notch, Shh,* and *Egf* signaling pathways). Thus, the primordial to primary follicle transition is a major transition and likely reflects the dramatic reorganization in follicle structure and initiation of growth and development. Of the 16 883 probe sets differentially detected between these stages, 5020 display a twofold change in relative abundance. Another apparent transition occurs between oocytes obtained from secondary follicles and those from small antral follicles, which corresponds to the acquisition of meiotic competence. The 736 probe sets of which ~65% are downregulated display a significant twofold change at this transition.

The principal component-based clustering shows three distinct patterns of gene expression. The first pattern shows consistent increase or decrease throughout the oocyte development and the most dramatic changes from the primordial to primary follicle stages, which the bulk of genes (10 117 probe sets) display (Fig. 3A). The second pattern peaks or hits the bottom at the primary follicle stage (Fig. 3B) and the third one shows the dynamic expression changes from the primary to the secondary follicle stages (Fig. 3C). The Expression Analysis Systematic Explorer software (http://david.abcc.ncifcrf.gov/ease/ease.jsp) for discovery of biological themes within the list of genes also shows the overrepresentation of genes involved in DNA repair and response to DNA damage throughout oocyte development, suggesting a protective mechanism to insure genomic integrity of the female germ line.

In addition, by analysis of global gene expression profiling of oocytes during the germinal vesicle stage to the metaphase II stage, new potential regulators and marker genes for oocyte maturation have been identified: *Pacsin2, Map2k* (Cui *et al.* 2007), and the genes related to BRCA1 regulation pathway, including *Bard1, Rbbp4, Brap, Rbbp7, Rbl2, Bub3,* and *Bub1b* (Gasca *et al.* 2007).

Global gene expression changes during loss of oocyte quality

To elucidate factors determining oocyte quality, a mouse model highlighting the age-related decline in fertility and oocyte quality was used (Hamatani *et al.* 2004*b*, Steuerwald *et al.* 2007). The expression profiles of metaphase II oocytes collected from 5- to 6-week-old mice were compared with those collected from 42- to 45-week-old mice using the NIA 60-mer oligo microarray (Hamatani *et al.* 2004*b*). Among ~11 000 genes whose transcripts were detected in oocytes, about 5% (530) showed statistically significant expression changes,

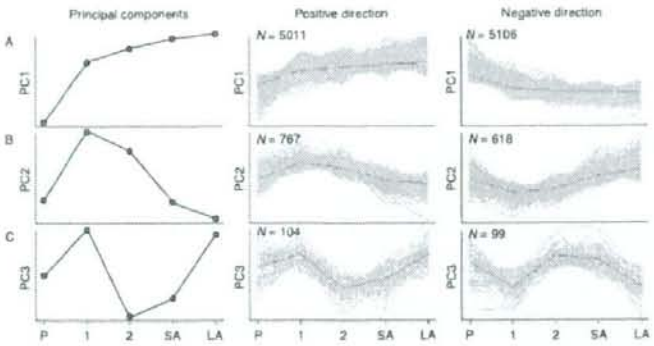

Figure 3 Principal component-based clustering to analyze gene expression profiles of oocytes during the primordial follicle stage to the large antral follicle stage (Pan *et al.* 2005) by NIA array analysis tool (http://lgsun.grc.nia.nih.gov/ANOVA/). The NIA Array Analysis tool identifies two clusters associated with a given pattern: genes positively and negatively correlated with the pattern. P, 1, 2, SA, and LA represent the primordial follicle stage, the primary follicle stage, the secondary follicle stage, the small antral follicle stage, and the large antral follicle stage respectively.

excluding the possibility of global decline in transcript abundance. Consistent with the generally accepted view of aging, the differentially expressed genes include ones involved in mitochondrial function and oxidative stress. Interestingly, a new non-invasive and highly sensitive method for measuring cellular respiration with scanning electrochemical microscopy shows that decreased cellular respiration in oocytes from aged mice is associated with impaired preimplantation development (Abe 2007). However, the expression of other genes involved in chromatin structure, DNA methylation, genome stability, and RNA helicases are also altered, suggesting the existence of additional mechanisms for aging in oocytes. For example, the decreased *Dnmt1* (*Dnmt1o* and *Dnmt1s*) expression and the increased *Dnmt3b* during aging are observed in oocytes. Because the same pattern of expression change in *Dnmt* genes has already been reported in aging WI-38 fibroblast cells (Lopatina *et al.* 2002), the genomic methylation patterns are suggested to be altered in aging cells. Telomerase reverse transcriptase and yeast mutant H/L/S mismatch repair gene homologs are also downregulated during aging. Interestingly, more than 30 zinc finger proteins are shown as the downregulated genes during aging. Furthermore, we identified and characterized a group of new oocyte-specific mouse genes, members of the human NACHT, leucine rich repeat and pyrin domain containing (*NALP/NLRP*) gene family among the transcripts decreased with aging. The *Nalp* gene family includes *Mater/Nalp5/Nlrp5* whose null mutant embryos arrest cleavage at the two-cell stage (Tong *et al.* 2000), suggesting an important role of this gene family in oogenesis, fertilization, and/or preimplantation development. These results have implications for aging research as well as for clinical ooplasmic donation to rejuvenate aging oocytes.

Polycystic ovary syndrome (PCOS) is another good model for studying loss of oocyte quality. The reproductive performance of women undergoing IVF treatment with PCOS is characterized by their good response to ovarian stimulation that yields higher number of oocytes; however, with lower implantation and higher miscarriage rates (Engmann *et al.* 1999, Ludwig *et al.* 1999, Mulders *et al.* 2003). Individual oocytes retrieved from nine women with PCOS and that from ten non-hirsute ovulatory women are used for microarray hybridization (Wood *et al.* 2007). Of the 8123 transcripts expressed in metaphase II oocytes, 374 show significant differences in mRNA abundance in the PCOS oocyte. The genes associated with chromosome alignment and centrosome, and the genes containing putative androgen receptors and/or PPARγ-binding sites are upregulated. The expression of these genes, which is generally not a part of the human oocyte transcriptome, is suggested to contribute to abnormalities in early embryonic development. Furthermore, upregulation of maternal-effect genes are notable. Although only seven mammalian maternal-effect genes (*Mater/Nlrp5*, *Hsf1*, *Dnmt1*, *Zar1*, *Npm2*, *Stella*, *Fmn2*, and *Bnc1*) have been identified to date, three (*Mater/Nlrp5*, *Fmn2*, and *Bnc1*) are upregulated. Increased expression of maternal-effect genes may negatively impact embryonic development.

Dielectrophoresis is a potential non-invasive method to select oocytes of good quality. In fact, dielectrophoretically separated *in vitro*-derived bovine metaphase II oocytes show a difference in the rate of blastocyst development and significant difference in transcriptional abundance of 36 genes as a result from global gene expression profiling. This suggests that dielectrophoretic behavior and the 36 genes including *Anxa2*, *Ptgs2*, and *Dnmt1* are potential biomarkers for oocyte quality (Dessie *et al.* 2007).

Recently, microarray technology was also applied to screening for chromosomal anomalies: comparative genomic hybridization (CGH) is used to assess the copy number of chromosomes in polar bodies and oocytes (Wells *et al.* 2002, Fragouli *et al.* 2006). CGH has the major advantage that every chromosome is tested, rather than the limited subset assessed using fluorescence *in situ* hybridization (FISH). The CGH protocols, which allow efficient DNA amplification from single cells and

reduce the amount of time required for the analysis, are currently undergoing preclinical testing in a number of preimplantation genetic diagnosis laboratories (Patrizio *et al.* 2007).

Identification of oocyte-specific transcripts and their clustering in the mouse genome

A mammalian oocyte is the only known cell that can activate a zygotic genome after fertilization and reprogram a somatic nucleus transferred from a differentiated cell in cloning experiments. Therefore, several genes specifically expressed in oocytes are likely responsible for the ability to reprogram genomes as well as for oogenesis. It is the case for the so-called maternal genes such as *Mater, Zar1*, and *Npm2* that are all required for normal embryonic development beyond the one-cell or two-cell stage (Fig. 4A; Tong *et al.* 2000, Dean 2002, Burns *et al.* 2003, Wu *et al.* 2003). *Gdf9* and *Bmp15* are also known to play important roles in female germ cells during folliculogenesis (Dong *et al.* 1996, Galloway *et al.* 2000). Accordingly, genes specifically expressed in the oocyte seem to control oogenesis, ovarian folliculogenesis, and preimplantation development.

In attempts to identify novel oocyte-specific genes, several groups have used mRNA differential display (Zeng & Schultz 2003), suppression subtractive hybridization (Hennebold *et al.* 2000), and *in silico* subtraction approaches (Rajkovic *et al.* 2001, Dade *et al.* 2003). It is, however, essential to analyze all transcripts/genes in a wide selection of organs and cell types including totipotent fertilized eggs, pluripotent embryonic cells, a variety of adult stem cells, and terminally differentiated cells. Sharov *et al.* (2003) obtained 249 200 high-quality EST sequences from the NCBI Unigene database that included a broad collection of NIA mouse cDNA libraries and clustered them into ~30 000 gene indexes including 977 previously unidentified genes. By analyzing the expression levels of the gene indexes based on the frequencies of the corresponding ESTs in Unigene cDNA libraries, genes that characterize oocytes and preimplantation embryos are identified (Sharov *et al.* 2003). Furthermore, the gene expression specificity to oocytes or/and preimplantation embryos is validated using gene expression profiling data of female germ cells during oogenesis and preimplantation embryos (Hamatani *et al.* 2004*a*, Wang *et al.* 2004, Pan *et al.* 2005). Several example of genes preferentially expressed in oocytes are selected and their gene expression levels are demonstrated to increase in oocytes during oogenesis (from the primordial follicle stage to the large antral follicle stage) and decrease during preimplantation development (from unfertilized egg to blastocyst) by the microarray experiments (Fig. 4B). Mager *et al.* (2006) also identified 51 genes as candidate maternal-effect genes *in silico* (always not present during the two-cell through the eight-cell or at the blastocyst stage), by comparing published results of three independent studies of mouse preimplantation embryo transcriptomes (Hamatani *et al.* 2004*a*, Wang *et al.* 2004, Zeng *et al.* 2004).

The group that found six genes of the mouse oogenesin family reported that not a few loci near the telomere in the mouse genome contain several genes specifically expressed in oocytes (Paillisson *et al.* 2005). Mouse oogenesin family genes are expressed exclusively in oocytes and present on chromosome 4 in a cluster of almost 1 Mb composed of 12 oogenesin paralogous genes. On the other hand, we also identified nine novel genes presenting similarities with *Mater/Nalp5* (Tong *et al.* 2000) and expression specific to oocytes, seven of which are clusterized on a certain locus of chromosome 7 (Fig. 5). The gene expression specificity of the novel Nalp-family genes to oocytes has been experimentally validated using Northern blot and *in situ* hybridization (Hamatani *et al.* 2004*b*, Fig. 6). Recently, we further identified a group of oocyte-specific genes encoding zinc finger proteins that clusterize in a near-telomere locus of chromosomes 6 and 11 (unpublished data). Telomeric regions of chromosomes are mainly composed of heterochromatin in most eukaryotic genomes. Because gene silencing near the telomere has been known and called 'telomere position effect' in *Drosophila* and yeast, the specific near-telomere position of the clusters of oocyte-specific genes in mice may contribute toward their gene silencing in non-ovarian tissues.

There is another noted attempt to identify important genes that are preferentially expressed in oocytes and conserved in chordates. Evsikov *et al.* (2006) compared the collection of ESTs from their mouse oocyte libraries to those from the eggs of *Xenopus* and ascidians to extract conserved genes that are expressed in chordate oocytes. More than 50% of the genes expressed in mouse oocyte libraries are also expressed in the eggs of *Xenopus* and ascidians. To investigate the evolutionary hardwired molecular pathways shared among chordates, GO term frequencies in 2090 genes that are commonly expressed in eggs of all three species are compared with those in the entire set of genes expressed in their mouse oocyte library. Although this analysis shows a substantial overlap with GO terms (biological process) associated with housekeeping genes, several GO terms (molecular function) such as 'motor activity,' 'small protein activating enzyme activity,' 'transferase activity,' 'helicase activity,' and two specific signal transducer activities (serine/threonine kinase activity and ligand-dependent nuclear receptor activity) are over-represented and provide a snapshot of gene functions shared particularly by the chordate oocytes. Another study group used a multi-species cDNA microarray containing 3456 transcripts from three distinct cDNA libraries from bovine, mouse, and *Xenopus* oocytes (Vallee *et al.* 2006). The cross-species hybridizations reveal that 1541 positive hybridization signals are generated by oocytes of all three species, and 268 of these, including *SMFN* (small fragment nuclease), *Spin* (spindlin), and

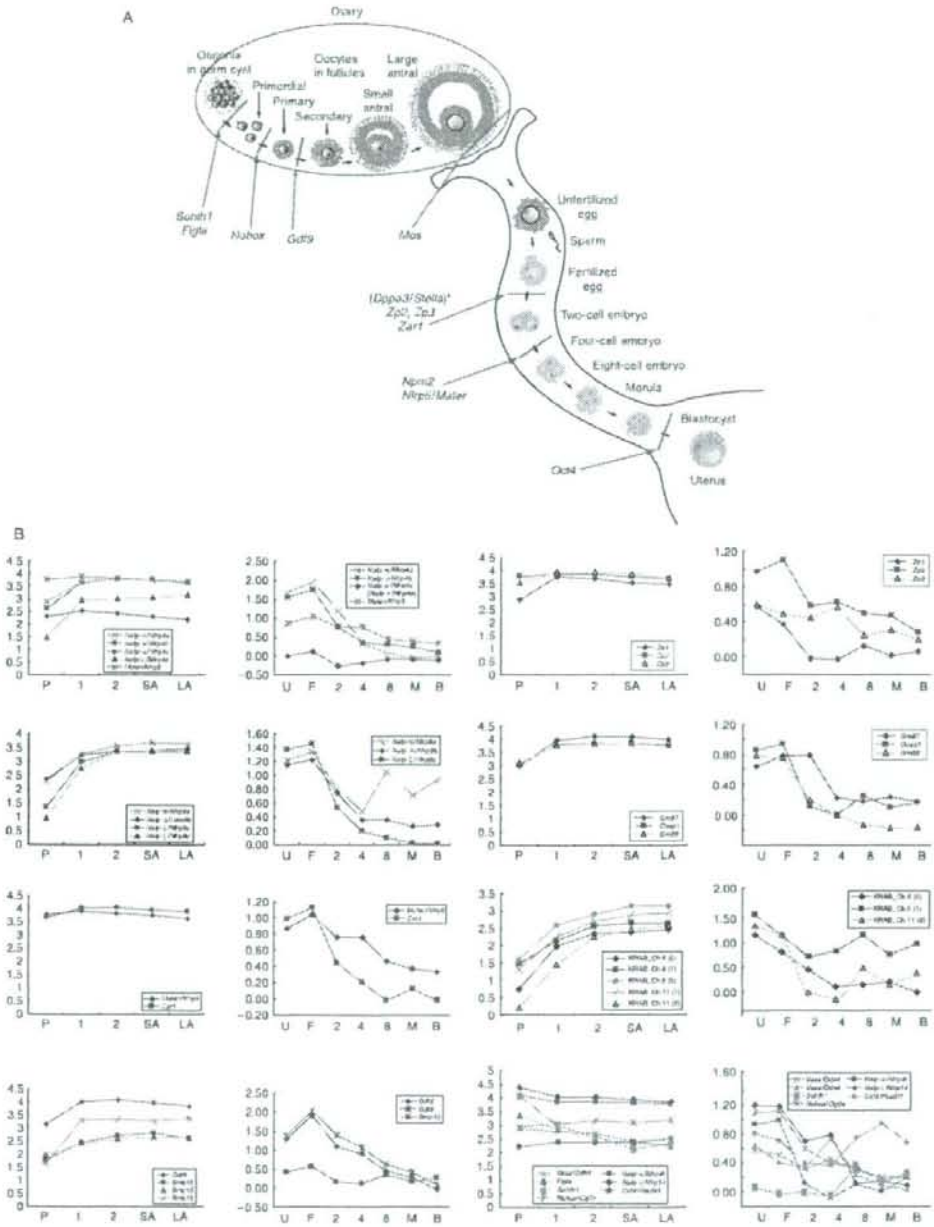

Figure 4 (A) Knockout mouse phenotypes of genes preferentially expressed in oocytes. *Development of embryos from *Stella*−/− intercrosses starts to be affected from 1.5 dpc onward (the two-cell stage) and only a low percentage reach the blastocyst stage by 3.5 dpc. (B) The gene expression changes of several genes known as oocyte specific. The oocyte-specific genes, including *Nalps*, showed increased expression during oogenesis and decreased expression during preimplantation development in the global gene expression studies. P, 1, 2, SA, and LA represent the primordial follicle stage, the primary follicle stage, the secondary follicle stage, the small antral follicle stage, and the large antral follicle stage respectively. U, F, 2, 4, 8, M, and B denote unfertilized egg, fertilized egg, two-cell embryo, four-cell embryo, eight-cell embryo, morula, and blastocyst respectively.

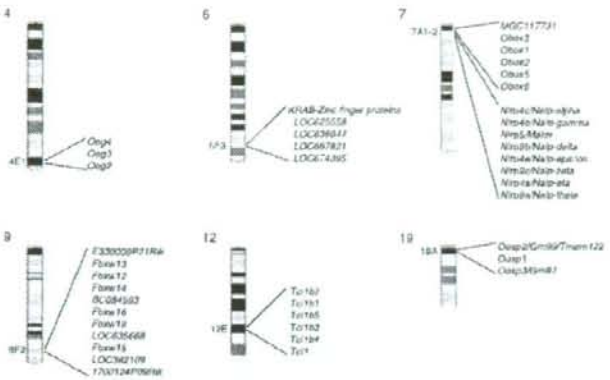

Figure 5 Clusters of oocyte-specific genes on mouse chromosomes 4, 6, 7, 9, 12, and 19.

PRMT1 (protein arginine methyltransferase 1) transcripts, are preferentially expressed in oocytes (Vallee *et al.* 2006). Furthermore, an important molecular characteristic of germ cells was also reported: germ cell-specific regulation of core promoter-associated transcription factors is conserved between *Xenopus* and mice (Xiao *et al.* 2006). *Tbpl2/Trf3* and *Gtf2a1l/Alf* are demonstrated to be expressed preferentially in oocytes and can form *in vitro* core promoter complexes with TBP and TFIIA. Therefore, identifying other germ cell-specific transcription factors is necessary to understand the genetic cascades that drive oocyte development and folliculogenesis.

Comparison of oocytes with ES cells in terms of their gene expression profiles

Recent studies on cell fusion between a somatic cell and an ES cell suggest that cytoplasm of ES cells can reprogram an introduced somatic nucleus to confer pluripotency. In this aspect, the cytoplasmic environments of ES cells and oocytes share the capacity to reprogram a somatic nucleus (Tada *et al.* 2001, Cowan *et al.* 2005). Accordingly, a set of genes commonly expressed in oocytes and ES cells are likely responsible for reprograming somatic cells. To identify these genes, gene expression profiling data of human oocytes and human ES cells were explored (Kocabas *et al.* 2006, Zhang *et al.* 2007). Compared with reference samples, 5331 and 1626 transcripts are significantly upregulated in human oocytes and ES cells respectively (Kocabas *et al.* 2006). When the genes differentially upregulated in human ES cells are intersected with those differentially upregulated in human oocytes, 388 transcripts are overlapped. This list of genes, including *POU5F1/OCT4*, *DNMT3b*, *DAZL*, and high-mobility group proteins (*HMGB2*, *HMGB3*, and *HMGN4*) (Kocabas *et al.* 2006), may provide good candidate genes for the future studies on molecular mechanisms of nuclear reprograming.

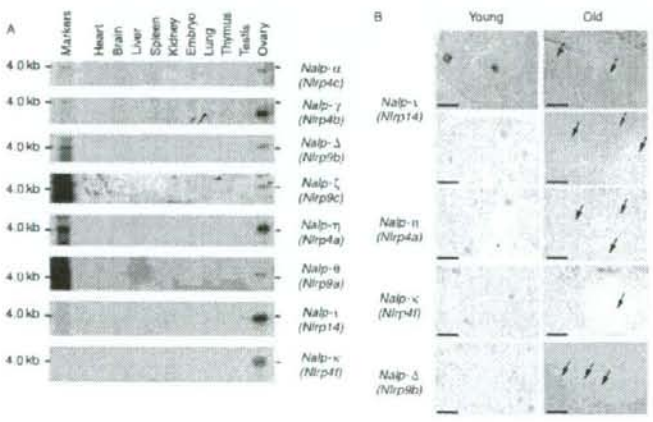

Figure 6 Oocyte-specific expression of the novel Nalp-family mouse genes (reprinted from 'Age-associated alteration of gene expression patterns in mouse oocytes', Hamatani T *et al.* 2004 *Human Molecular Genetics* **13** 2263–2278, with permission from Oxford University Press). (A) Northern blot analysis shows their ovary-specific expression and (B) *in situ* hybridization shows their oocyte-specific expression on ovary sections.

On the other hand, 'induced pluripotent stem cells (iPS cells)' were recently generated by forced expression of defined factors: *Pou5f1/Oct4*, *Sox2*, *Klf4*, and *Myc* (Takahashi & Yamanaka 2006). Surprisingly, iPS cells selected by Nanog expression are capable of germ cell transmission (Okita *et al.* 2007). These iPS factors, however, show little maternal expression in oocytes (except in the case of *Oct4*) and increased zygotic expression during preimplantation stages (except in the case of *Myc*), based on EST frequencies in Unigene cDNA libraries and microarray data during oogenesis to preimplantation development (Fig. 7). Therefore, the mechanism of oocytes to induce pluripotency is likely different from that of ES cells. Although the genes commonly expressed in oocytes and ES cells are not necessarily important to induce pluripotency, maternal factors that can induce zygotic expression of the 'iPS factors' (*Oct4*, *Sox2*, and *Klf4*) are rather more substantial in oocytes.

Perspective

Oocytes offer a relatively homogeneous biological system that is well adapted to gene expression profiling studies: arrest of cell cycle at the metaphase II stage, quiescence in transcription after germinal vesicle breakdown, and little contamination in oocyte samples with any other types of cells after thorough removal of cumulus cells. There are, however, several limitations in applying microarray technologies to study the molecular mechanisms in oocytes and preimplantation embryos. Although the recent advent of linear RNA amplification (*in vitro* transcription-based protocols) and exponential amplification (PCR-based strategies) techniques allowed several groups to study oocyte transcriptomes using a tiny amount of RNA even in an individual oocyte (Bermudez *et al.* 2004, Dobson *et al.* 2004, Li *et al.* 2006, Jones *et al.* 2007), the efficacy of RNA amplification is not yet good enough to analyze an individual blastomere of preimplantation embryos. Furthermore, poly(A) length affects efficiency of RNA amplification. Although the synthesis of new transcripts essentially ceases after germinal vesicle breakdown, poly(A) tails of some classes of existing transcripts in oocytes are elongated, leading to increased translation and protein levels (Bachvarova 1992). Thus, regulation of the poly(A) tail length is a major mechanism for controlling maternal transcript activity. Unlike the T7-oligo(dT) primers used in the conventional linear RNA amplification procedures, the uniquely designed Full Spectrum MultiStart Primers for *in vitro* transcription from System Biosciences (Mountain View, CA, USA) initiates cDNA synthesis at multiple points along mRNAs with little or no bias with respect to the length of poly(A) tails. Transcript profiles generated from microarray studies using this modified RNA amplification protocol would provide a more accurate perspective of the

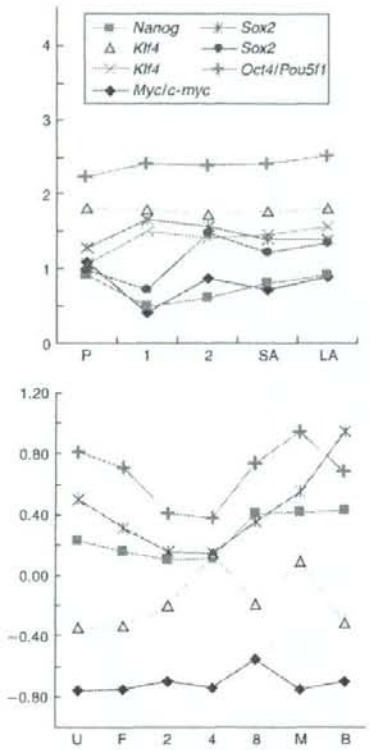

Figure 7 The gene expression changes of the iPS factors based on the published microarray data. P, 1, 2, SA, and LA represent the primordial follicle stage, the primary follicle stage, the secondary follicle stage, the small antral follicle stage, and the large antral follicle stage respectively. U, F, 2, 4, 8, M, and B denote unfertilized egg, fertilized egg, two-cell embryo, four-cell embryo, eight-cell embryo, morula, and blastocyst respectively.

global changes in populations of both degrading and stable transcripts during oocyte maturation and ZGA (Su *et al.* 2007).

'Tailor-made regenerative medicine' includes nuclear transfer from a patient's somatic cell to an enucleated donated oocyte, development of the reconstructed embryo up to the blastocyst stage, and establishment of the patient's ES cells. 'Making oocytes' will be an essential technique to develop 'tailor-made regenerative medicine' that needs large quantities of healthy ooplasms. 'Oocyte-like' cells were recently grown and isolated by utilizing GFP expression as a selection marker during differentiation of ES cells containing GFP expression cassettes under the *Pou5f1* promoter (Hubner *et al.* 2003). Nobody, however, has succeeded in generating oocytes by manipulating gene expression in ES and somatic cells. Even though forced expression of a set of several transcription factors in ES cells

may allow us to generate an oocyte, there is a problem in the oocyte; its nucleus ought to have genetic abnormalities. In contrast, its ooplasm might contain all the gene products that can support embryonic development after fertilization. Unlike another strategy using iPS cells that cannot avoid transmitting genetic abnormalities, the ooplasm can be safely used for 'tailor-made regenerative medicine' or 'ooplasmic donation'.

Since transcriptional cascades that activate an oocyte-specific developmental program are largely unknown, a set of master genes that drive the cascades have not yet been defined. Oocyte-specific transcription factors, however, are likely to be the critical switches for the differentiation into oocytes and good candidates for manipulation of gene expression. For example, NOBOX binds to the NOBOX binding elements with high affinity and augments transcriptional activity of mouse *Pou5f1* and *Gdf9* promoters (Choi & Rajkovic 2006). Other examples are factor in germ cell (FIGLA) and SOHLH1 that bind to E-box. They are suggested to increase transcriptional activity of *Zp1–3*, which have promoters including E-box (Yan *et al.* 2006: Pangas, 2006 #613).

On the other hand, nobody pays attention to a transcription factor whose knockout showed no distinctive phenotypes. Nonetheless, recent advent in microarray technologies allows us to catch any changes in a gene expression profile of cells transfected with a construct to modify gene expression. If a gene expression profile of ES cells approaches that of oocytes in the PCA coordinate, in spite of no phenotypic change, by upregulation of a certain transcription factor, the transcription factor is likely a candidate gene as a tool to induce the oocyte developmental program (Fig. 8). Further forced expression of another transcription factor in the ES cell may result in a similar gene expression profile to that of oocytes and then may achieve a certain remarkable phenotype including follicles or oocytes. Such synergy between cell biology and bioinformatics will become more important and beneficial to establish an *in vitro* oocyte-development model to 'make an oocyte'.

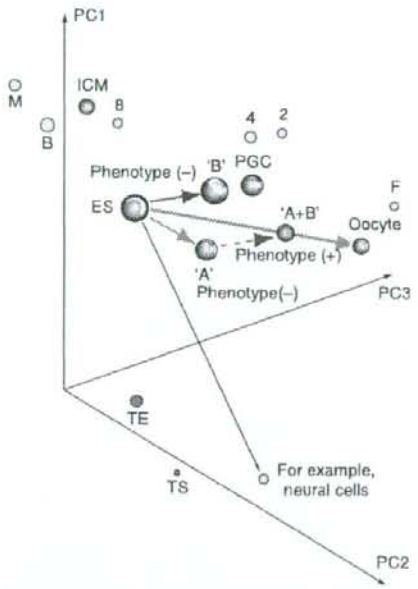

Figure 8 Explanation of a model to transform ES cells efficiently into oocytes using gene expression profiling as a guide. PC, principle component; PGC, primordial germ cell; ICM, inner cell mass; TE, trophectoderm; F, fertilized egg; 2, two-cell embryo; 4, four-cell embryo; 8, eight-cell embryo; M, morula; B, blastocyst. If over-expression of 'gene A' makes a global expression profile of ES cells closer to that of oocytes in the PCA coordinate, 'gene A' could be a good candidate to promote the oocyte developmental program. Even though no changes in phenotypes of ES cells are observed with over-expression of 'gene A', forced expression of 'gene A' plus that of 'gene B' in ES cells may show a distinctive phenotype including oocytes or follicles.

Acknowledgements

The authors declare that there is no conflict of interest that would prejudice the impartiality of this scientific work.

References

Abe H 2007 A non-invasive and sensitive method for measuring cellular respiration with a scanning electrochemical microscopy to evaluate embryo quality. *Journal of Mammalian Ova Research* **24** 70–78.

Adjaye J 2005 Whole-genome approaches for large-scale gene identification and expression analysis in mammalian preimplantation embryos. *Reproduction, Fertility, and Development* **17** 37–45.

Armstrong DT 2001 Effects of maternal age on oocyte developmental competence. *Theriogenology* **55** 1303–1322.

Ashburner M, Ball CA, Blake JA, Botstein D, Butler H, Cherry JM, Davis AP, Dolinski K, Dwight SS, Eppig JT, *et al.* 2000 Gene ontology: tool for the unification of biology. The Gene Ontology Consortium. *Nature Genetics* **25** 25–29.

ASRM/SART 2000 Assisted reproductive technology in the United States: 1997 results generated from the American Society for Reproductive Medicine/Society for Assisted Reproductive Technology Registry. *Fertility and Sterility* **74** 641–653 (discussion 653–644).

Assou S, Anahory T, Pantesco V, Le Carrour T, Pellestor F, Klein B, Reyftmann L, Dechaud H, De Vos J & Hamamah S 2006 The human cumulus–oocyte complex gene-expression profile. *Human Reproduction* **21** 1705–1719.

Bachvarova RF 1992 A maternal tail of poly(A): the long and the short of it. *Cell* **69** 895–897.

Bermudez MG, Wells D, Malter H, Munne S, Cohen J & Steuerwald NM 2004 Expression profiles of individual human oocytes using microarray technology. *Reproductive Biomedicine Online* **8** 325–337.

Burns KH, Viveiros MM, Ren Y, Wang P, DeMayo FJ, Frail DE, Eppig JJ & Matzuk MM 2003 Roles of NPM2 in chromatin and nucleolar organization in oocytes and embryos. *Science* **300** 633–636.

Carter MG, Hamatani T, Sharov AA, Carmack CE, Qian Y, Aiba K, Ko NT, Dudekula DB, Brzoska PM, Hwang SS, *et al.* 2003 *In situ*-synthesized novel microarray optimized for mouse stem cell and early developmental expression profiling. *Genome Research* **13** 1011–1021.

Choi Y & Rajkovic A 2006 Characterization of NOBOX DNA binding specificity and its regulation of Gdf9 and Pou5f1 promoters. *Journal of Biological Chemistry* **281** 35747–35756.

Cohen J, Scott R, Schimmel T, Levron J & Willadsen S 1997 Birth of infant after transfer of anucleate donor oocyte cytoplasm into recipient eggs. *Lancet* **350** 186–187.

Cohen J, Scott R, Alikani M, Schimmel T, Munne S, Levron J, Wu L, Brenner C, Warner C & Willadsen S 1998 Ooplasmic transfer in mature human oocytes. *Molecular Human Reproduction* **4** 269–280.

Cowan CA, Atienza J, Melton DA & Eggan K 2005 Nuclear reprogramming of somatic cells after fusion with human embryonic stem cells. *Science* **309** 1369–1373.

Cui XS, Li XY, Yin XJ, Kong IK, Kang JJ & Kim NH 2007 Maternal gene transcription in mouse oocytes: genes implicated in oocyte maturation and fertilization. *Journal of Reproduction and Development* **53** 405–418.

Dade S, Callebaut I, Mermillod P & Monget P 2003 Identification of a new expanding family of genes characterized by atypical LRR domains. Localization of a cluster preferentially expressed in oocyte. *FEBS Letters* **555** 533–538.

Dahlquist KD, Salomonis N, Vranizan K, Lawlor SC & Conklin BR 2002 GenMAPP, a new tool for viewing and analyzing microarray data on biological pathways. *Nature Genetics* **31** 19–20.

Dean J 2002 Oocyte-specific genes regulate follicle formation, fertility and early mouse development. *Journal of Reproductive Immunology* **53** 171–180.

Dessie SW, Rings F, Holker M, Gilles M, Jennen D, Tholen E, Havlicek V, Besenfelder U, Sukhorukov VL, Zimmermann U, *et al.* 2007 Dielectrophoretic behavior of *in vitro*-derived bovine metaphase II oocytes and zygotes and its relation to *in vitro* embryonic developmental competence and mRNA expression pattern. *Reproduction* **133** 931–946.

Dobson AT, Raja R, Abeyta MJ, Taylor T, Shen S, Haqq C & Pera RA 2004 The unique transcriptome through day 3 of human preimplantation development. *Human Molecular Genetics* **13** 1461–1470.

Dong J, Albertini DF, Nishimori K, Kumar TR, Lu N & Matzuk MM 1996 Growth differentiation factor-9 is required during early ovarian folliculogenesis. *Nature* **383** 531–535.

Doniger SW, Salomonis N, Dahlquist KD, Vranizan K, Lawlor SC & Conklin BR 2003 MAPPFinder: using gene ontology and GenMAPP to create a global gene-expression profile from microarray data. *Genome Biology* **4** R7.

Engmann L, Maconochie N, Sladkevicius P, Bekir J, Campbell S & Tan SL 1999 The outcome of *in vitro* fertilization treatment in women with sonographic evidence of polycystic ovarian morphology. *Human Reproduction* **14** 167–171.

Evsikov AV, Graber JH, Brockman JM, Hampl A, Holbrook AE, Singh P, Eppig JJ, Solter D & Knowles BB 2006 Cracking the egg: molecular dynamics and evolutionary aspects of the transition from the fully grown oocyte to embryo. *Genes and Development* **20** 2713–2727.

Fragouli E, Wells D, Thornhill A, Serhal P, Faed MJ, Harper JC & Delhanty JD 2006 Comparative genomic hybridization analysis of human oocytes and polar bodies. *Human Reproduction* **21** 2319–2328.

Galloway SM, McNatty KP, Cambridge LM, Laitinen MP, Juengel JL, Jokiranta TS, McLaren RJ, Luiro K, Dodds KG, Montgomery GW, *et al.* 2000 Mutations in an oocyte-derived growth factor gene (BMP15) cause increased ovulation rate and infertility in a dosage-sensitive manner. *Nature Genetics* **25** 279–283.

Gasca S, Pellestor F, Assou S, Loup V, Anahory T, Dechaud H, De Vos J & Hamamah S 2007 Identifying new human oocyte marker genes: a microarray approach. *Reproductive Biomedicine Online* **14** 175–183.

Hamatani T, Carter MG, Sharov AA & Ko MS 2004*a* Dynamics of global gene expression changes during mouse preimplantation development. *Developmental Cell* **6** 117–131.

Hamatani T, Falco G, Carter MG, Akutsu H, Stagg CA, Sharov AA, Dudekula DB, VanBuren V & Ko MS 2004*b* Age-associated alteration of gene expression patterns in mouse oocytes. *Human Molecular Genetics* **13** 2263–2278.

Hennebold JD, Tanaka M, Saito J, Hanson BR & Adashi EY 2000 Ovary-selective genes I: the generation and characterization of an ovary-selective complementary deoxyribonucleic acid library. *Endocrinology* **141** 2725–2734.

Hodgman R, Tay J, Mendez R & Richter JD 2001 CPEB phosphorylation and cytoplasmic polyadenylation are catalyzed by the kinase IAK1/Eg2 in maturing mouse oocytes. *Development* **128** 2815–2822.

Hubner K, Fuhrmann G, Christenson LK, Kehler J, Reinbold R, De La Fuente R, Wood J, Strauss JF III, Boiani M & Scholer HR 2003 Derivation of oocytes from mouse embryonic stem cells. *Science* **300** 1251–1256.

Hughes TR, Mao M, Jones AR, Burchard J, Marton MJ, Shannon KW, Lefkowitz SM, Ziman M, Schelter JM, Meyer MR, *et al.* 2001 Expression profiling using microarrays fabricated by an ink-jet oligonucleotide synthesizer. *Nature Biotechnology* **19** 342–347.

Johnson MH, Lim A, Fernando D & Day ML 2002 Circadian clockwork genes are expressed in the reproductive tract and conceptus of the early pregnant mouse. *Reproductive Biomedicine Online* **4** 140–145.

Jones GM, Song B, Cram DS & Trounson AO 2007 Optimization of a microarray based approach for deriving representative gene expression profiles from human oocytes. *Molecular Reproduction and Development* **74** 8–17.

Klein J & Sauer MV 2001 Assessing fertility in women of advanced reproductive age. *American Journal of Obstetrics and Gynecology* **185** 758–770.

Ko MS 2004 Embryogenomics of pre-implantation mammalian development: current status. *Reproduction, Fertility, and Development* **16** 79–85.

Ko MS, Kitchen JR, Wang X, Threat TA, Hasegawa A, Sun T, Grahovac MJ, Kargul GJ, Lim MK, Cui Y, *et al.* 2000 Large-scale cDNA analysis reveals phased gene expression patterns during preimplantation mouse development. *Development* **127** 1737–1749.

Kocabas AM, Crosby J, Ross PJ, Otu HH, Beyhan Z, Can H, Tam WL, Rosa GJ, Halgren RG, Lim B, *et al.* 2006 The transcriptome of human oocytes. *PNAS* **103** 14027–14032.

van Kooij RJ, Looman CW, Habbema JD, Dorland M & te Velde E 1996 Age-dependent decrease in embryo implantation rate after *in vitro* fertilization. *Fertility and Sterility* **66** 769–775.

Li SS, Liu YH, Tseng CN & Singh S 2006 Analysis of gene expression in single human oocytes and preimplantation embryos. *Biochemical and Biophysical Research Communications* **340** 48–53.

Lopatina N, Haskell JF, Andrews LG, Poole JC, Saldanha S & Tollefsbol T 2002 Differential maintenance and de novo methylating activity by three DNA methyltransferases in aging and immortalized fibroblasts. *Journal of Cellular Biochemistry* **84** 324–334.

Ludwig M, Finas DF, al-Hasani S, Diedrich K & Ortmann O 1999 Oocyte quality and treatment outcome in intracytoplasmic sperm injection cycles of polycystic ovarian syndrome patients. *Human Reproduction* **14** 354–358.

Mager J, Schultz RM, Brunk BP & Bartolomei MS 2006 Identification of candidate maternal-effect genes through comparison of multiple microarray data sets. *Mammalian Genome* **17** 941–949.

Mendez R & Richter JD 2001 Translational control by CPEB: a means to the end. *Nature Reviews. Molecular Cell Biology* **2** 521–529.

Mulders AG, Laven JS, Imani B, Eijkemans MJ & Fauser BC 2003 IVF outcome in anovulatory infertility (WHO group 2) – including polycystic ovary syndrome – following previous unsuccessful ovulation induction. *Reproductive Biomedicine Online* **7** 50–58.

Navot D, Bergh PA, Williams MA, Garrisi GJ, Guzman I, Sandler B & Grunfeld L 1991 Poor oocyte quality rather than implantation failure as a cause of age-related decline in female fertility. *Lancet* **337** 1375–1377.

Nothias JY, Majumder S, Kaneko KJ & DePamphilis ML 1995 Regulation of gene expression at the beginning of mammalian development. *Journal of Biological Chemistry* **270** 22077–22080.

Okita K, Ichisaka T & Yamanaka S 2007 Generation of germline-competent induced pluripotent stem cells. *Nature* **448** 313–317.

Paillisson A, Dade S, Callebaut I, Bontoux M, Dalbies-Tran R, Vaiman D & Monget P 2005 Identification, characterization and metagenome analysis of oocyte-specific genes organized in clusters in the mouse genome. *BMC Genomics* **6** 76.

Pan H, O'Brien MJ, Wigglesworth K, Eppig JJ & Schultz RM 2005 Transcript profiling during mouse oocyte development and the effect of gonadotropin priming and development *in vitro*. *Developmental Biology* **286** 493–506.

Patrizio P, Fragouli E, Bianchi V, Borini A & Wells D 2007 Molecular methods for selection of the ideal oocyte. *Reproductive Biomedicine Online* **15** 346–353.

Rajkovic A, Yan MSC, Klysik M & Matzuk M 2001 Discovery of germ cell-specific transcripts by expressed sequence tag database analysis. *Fertility and Sterility* **76** 550–554.

Schultz RM 2002 The molecular foundations of the maternal to zygotic transition in the preimplantation embryo. *Human Reproduction Update* **8** 323–331.

Sharov AA, Piao Y, Matoba R, Dudekula DB, Qian Y, VanBuren V, Falco G, Martin PR, Stagg CA, Bassey UC, *et al.* 2003 Transcriptome analysis of mouse stem cells and early embryos. *PLoS Biology* **1** E74.

Steuerwald NM, Bermudez MG, Wells D, Munne S & Cohen J 2007 Maternal age-related differential global expression profiles observed in human oocytes. *Reproductive Biomedicine Online* **14** 700–708.

Su YQ, Sugiura K, Woo Y, Wigglesworth K, Kamdar S, Affourtit J & Eppig JJ 2007 Selective degradation of transcripts during meiotic maturation of mouse oocytes. *Developmental Biology* **302** 104–117.

Suzumori N, Burns KH, Yan W & Matzuk MM 2003 RFPL4 interacts with oocyte proteins of the ubiquitin-proteasome degradation pathway. *PNAS* **100** 550–555.

Tada M, Takahama Y, Abe K, Nakatsuji N & Tada T 2001 Nuclear reprogramming of somatic cells by *in vitro* hybridization with ES cells. *Current Biology* **11** 1553–1558.

Takahashi K & Yamanaka S 2006 Induction of pluripotent stem cells from mouse embryonic and adult fibroblast cultures by defined factors. *Cell* **126** 663–676.

Takeuchi T, Ergun B, Huang TH, Rosenwaks Z & Palermo GD 1999 A reliable technique of nuclear transplantation for immature mammalian oocytes. *Human Reproduction* **14** 1312–1317.

Terada Y, Simerly C & Schatten G 2000 Microfilament stabilization by jasplakinolide arrests oocyte maturation, cortical granule exocytosis, sperm incorporation cone resorption, and cell-cycle progression, but not DNA replication, during fertilization in mice. *Molecular Reproduction and Development* **56** 89–98.

Tong ZB, Gold L, Pfeifer KE, Dorward H, Lee E, Bondy CA, Dean J & Nelson LM 2000 Mater, a maternal effect gene required for early embryonic development in mice. *Nature Genetics* **26** 267–268.

Vallee M, Robert C, Methot S, Palin MF & Sirard MA 2006 Cross-species hybridizations on a multi-species cDNA microarray to identify evolutionarily conserved genes expressed in oocytes. *BMC Genomics* **7** 113.

Wang QT, Piotrowska K, Ciemerych MA, Milenkovic L, Scott MP, Davis RW & Zernicka-Goetz M 2004 A genome-wide study of gene activity reveals developmental signaling pathways in the preimplantation mouse embryo. *Developmental Cell* **6** 133–144.

Wells D, Escudero T, Levy B, Hirschhorn K, Delhanty JD & Munne S 2002 First clinical application of comparative genomic hybridization and polar body testing for preimplantation genetic diagnosis of aneuploidy. *Fertility and Sterility* **78** 543–549.

Wood JR, Dumesic DA, Abbott DH & Strauss JF III 2007 Molecular abnormalities in oocytes from women with polycystic ovary syndrome revealed by microarray analysis. *Journal of Clinical Endocrinology and Metabolism* **92** 705–713.

Wu X, Viveiros MM, Eppig JJ, Bai Y, Fitzpatrick SL & Matzuk MM 2003 Zygote arrest 1 (Zar1) is a novel maternal-effect gene critical for the oocyte-to-embryo transition. *Nature Genetics* **33** 187–191.

Xiao L, Kim M & DeJong J 2006 Developmental and cell type-specific regulation of core promoter transcription factors in germ cells of frogs and mice. *Gene Expression Patterns* **6** 409–419.

Yan C, Elvin JA, Lin YN, Hadsell LA, Wang J, DeMayo FJ & Matzuk MM 2006 Regulation of growth differentiation factor 9 expression in oocytes *in vivo*: a key role of the E-box. *Biology of Reproduction* **74** 999–1006.

Yoon SJ, Kim KH, Chung HM, Choi DH, Lee WS, Cha KY & Lee KA 2006 Gene expression profiling of early follicular development in primordial, primary, and secondary follicles. *Fertility and Sterility* **85** 193–203.

Zeng F & Schultz RM 2003 Gene expression in mouse oocytes and preimplantation embryos: use of suppression subtractive hybridization to identify oocyte- and embryo-specific genes. *Biology of Reproduction* **68** 31–39.

Zeng F, Baldwin DA & Schultz RM 2004 Transcript profiling during preimplantation mouse development. *Developmental Biology* **272** 483–496.

Zhang P, Kerkela E, Skottman H, Levkov L, Kivinen K, Lahesmaa R, Hovatta O & Kere J 2007 Distinct sets of developmentally regulated genes that are expressed by human oocytes and human embryonic stem cells. *Fertility and Sterility* **87** 677–690.

Received 22 September 2007
First decision 31 October 2007
Revised manuscript received 1 February 2008
Accepted 27 February 2008

The fusing ability of sperm is bestowed by CD9-containing vesicles released from eggs in mice

Kenji Miyado*†‡§, Keiichi Yoshida‡¶, Kazuo Yamagata‖, Keiichi Sakakibara*, Masaru Okabe**, Xiaobiao Wang*, Kiyoko Miyamoto*, Hidenori Akutsu*, Takahiko Kondo*, Yuji Takahashi*, Tadanobu Ban††, Chizuru Ito¶, Kiyotaka Toshimori¶, Akihiro Nakamura*, Masahiko Ito*, Mami Miyado*, Eisuke Mekada**, and Akihiro Umezawa*

*National Center for Child Health and Development, 2-10-1 Okura, Setagaya, Tokyo 157-8535, Japan; †School of Biomedical Science, Tokyo Medical and Dental University, Yushima, Bunkyo, Tokyo 113-8510, Japan; §Graduate School of Medicine, Chiba University, 1-8-1 Inohana, Chuo-ku, Chiba 260-8670, Japan; ‖Center for Developmental Biology, RIKEN Kobe Institute, 2-2-3 Minatojima-minamimachi, Chuo-ku, Kobe, Hyogo 650-0047, Japan; and **Research Institute for Microbial Diseases, and ††Faculty of Medicine, Osaka University, 3-1 Yamadaoka, Suita, Osaka 565-0871, Japan

Edited by Ryuzo Yanagimachi, University of Hawaii, Honolulu, HI, and approved July 8, 2008 (received for review November 8, 2007)

Membrane fusion is an essential step in the encounter of two nuclei from sex cells—sperm and egg—in fertilization. However, aside from the involvement of two molecules, CD9 and Izumo, the mechanism of fusion remains unclear. Here, we show that sperm–egg fusion is mediated by vesicles containing CD9 that are released from the egg and interact with sperm. We demonstrate that the $CD9^{-/-}$ eggs, which have a defective sperm-fusing ability, have impaired release of CD9-containing vesicles. We investigate the fusion-facilitating activity of CD9-containing vesicles by examining the fusion of sperm to $CD9^{-/-}$ eggs with the aid of exogenous CD9-containing vesicles. Moreover, we show, by examining the fusion of sperm to $CD9^{-/-}$ eggs, that hamster eggs have a similar fusing ability as mouse eggs. The CD9-containing vesicle release from unfertilized eggs provides insight into the mechanism required for fusion with sperm.

fertilization | membrane fusion | EGFP | exosome

Fertilization is an essential process that naturally produces a cell capable of developing into a new individual. It consists of sequential events, including membrane fusion of sperm and egg (1). Despite the importance of understanding fertilization in controlling human reproduction and preserving endangered species, the molecular basis underlying the fusion remains a mystery, however. Previously, we reported that a tetraspan-membrane protein (tetraspanin), CD9, is expressed on the egg plasma membrane and is required for sperm–egg fusion (2–4). A role of CD9 in other fusion events also has been demonstrated (5). When sperm are added to eggs from $CD9^{-/-}$ females, the sperm bind to the egg plasma membrane normally, but fusion is severely impaired (2–4). Two recent observations suggest that CD9 plays a role in the organization of egg membrane. First, CD9 is transferred from the egg to the fertilizing sperm present in the perivitelline space (PVS) (6), suggesting the involvement of a process similar to trogocytosis, a mechanism of cell-to-cell contact-dependent transfer of membrane fragments (7). Second, CD9 deficiency alters the length and density of microvilli on the egg plasma membrane (8). CD9 is also known to be a component of exosomes, membrane vesicles released from a wide range of cells (9, 10). Despite its relationship to CD9, the involvement of exosome release in sperm–egg fusion remains unknown. In the present study, we analyzed the potential of enhanced green fluorescent protein (EGFP)-tagged CD9 (CD9-EGFP) as a reporter protein to study sperm–egg fusion in living mouse eggs.

Results

To observe the movement of CD9 during sperm–egg fusion, we generated a transgenic mouse line that expressed CD9-EGFP only in eggs (Fig. 1*A*), and converted to the genetic background of $CD9^{-/-}$ mice by mating mice. Western blot analysis using anti-CD9 monoclonal antibody (mAb) revealed that an expected CD9-EGFP with a molecular mass of 51 kDa (CD9 and EGFP contributing to 24 and 27 kDa, respectively) was expressed in the eggs collected from $Tg^{+}CD9^{-/-}$ mice; however, the amount of CD9-EGFP expressed in $CD9^{-/-}$ eggs was estimated to be 10% of that of endogenous CD9 in the $CD9^{+/+}$ eggs (Fig. 1*B*). Despite the small amount of CD9-EGFP expressed in eggs, CD9-EGFP demonstrated the ability to reverse the sterility of $CD9^{-/-}$ females (Fig. 1*C*). The numbers of pups obtained from $Tg^{+}CD9^{-/-}$ females (6.4 ± 0.5) were similar to those from

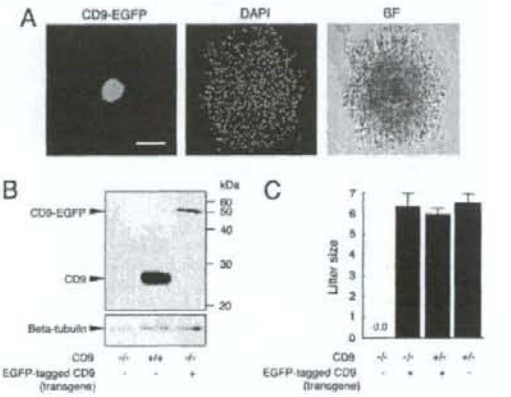

Fig. 1. Generation of mice expressing CD9-EGFP in eggs. (*A*) CD9-EGFP specifically expressed in eggs with mouse ZP3-promoter. Cumulus oocyte complex from $Tg^{+}CD9^{-/+}$ oviducts was collected at 14 h after injection of human chorionic gonadotropin. Nuclei of an egg and cumulus cells were counterstained with DAPI. (*Left*) CD9-EGFP. (*Center*) DAPI. (*Right*) Bright field. Scale bar: 100 μm. (*B*) Western blot analysis for eggs collected from $CD9^{-/-}$, $CD9^{+/+}$, and $Tg^{+}CD9^{-/-}$ mice. The same amounts, including 30 eggs of each lysate, were examined by anti-CD9 and anti-beta-tubulin mAbs (internal control). (*C*) Litter sizes of $CD9^{-/-}$ (n = 31), $Tg^{+}CD9^{-/-}$ (n = 35), $Tg^{+}CD9^{+/-}$ (n = 16), and $CD9^{+/-}$ mice (n = 15) (mean ± SEM). The numbers of females examined are in parentheses.

Author contributions: K. Miyado, K. Yamagata, M.O., and A.U. designed research; K. Miyado, K. Yoshida, K.S., X.W., K. Miyamoto, H.A., T.K., Y.T., T.B., C.I., A.N., M.I., and M.M. performed research; K. Miyado contributed new reagents/analytic tools; K. Miyado, K. Yoshida, H.A., K.T., E.M., and A.U. analyzed data; and K. Miyado wrote the paper.

The authors declare no conflicts of interest.

This article is a PNAS Direct Submission.

Freely available online through the PNAS open access option.

‡K. Miyado and K. Yoshida contributed equally to this work.

§To whom correspondence should be addressed. E-mail: kmiyado@nch.go.jp.

This article contains supporting information online at www.pnas.org/cgi/content/full/0710608105/DCSupplemental.

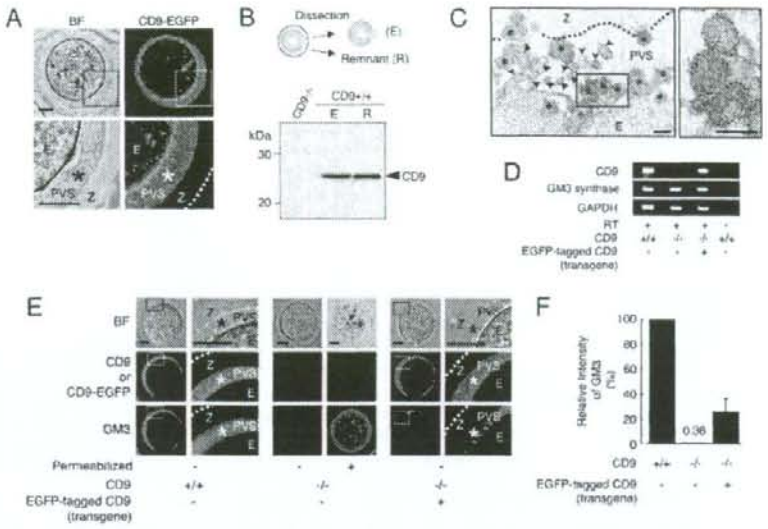

Fig. 2. Identification of secretory vesicles containing CD9 from unfertilized eggs. *A*, A single confocal image showing CD9-EGFP in unfertilized $Tg^{+}CD9^{-/-}$ eggs (E), including the PVS (*), zona pellucida (Z), and the outer margin of the zona pellucida (dotted line). (*Left*) Bright field. (*Right*) CD9-EGFP. *Lower* are enlarged images of the boxed areas. (*B*) Western blot analysis for eggs mechanically fractionated as shown in the diagram: zona-intact $CD9^{-/-}$ eggs (E) (10 eggs per lane) and zona-free $CD9^{+/+}$ eggs (10 eggs per lane). The medium (R) containing the remnant material from 40 eggs treated with a piezo manipulator was loaded in each lane. (*C*) Immunoelectron-microscopic analysis of $CD9^{+/+}$ eggs. The zona-intact $CD9^{-/+}$ eggs were examined using anti-CD9-mAb and 5-nm gold beads conjugated with anti-rat IgG Ab. Left panel: Image including CD9-containing vesicles (*), microvilli (arrowheads), zona pellucida (Z), perivitelline space (PVS), and egg (E). (*Right*) An enlarged image of the boxed region in the left panel. Scale bar: 200 nm. (*D*) RT-PCR for CD9, GM3 synthase, and glyceraldehyde-3-phosphate dehydrogenase transcripts in $CD9^{+/+}$, $CD9^{-/-}$, and $Tg^{+}CD9^{-/-}$ eggs. The same amounts, including 50 eggs in each reaction, were examined. The right end lanes are negative controls in which RT was removed from reactions of wild-type eggs. (*E*) Localization of GM3 and CD9 in $CD9^{+/+}$, $CD9^{-/-}$, and $Tg^{+}CD9^{-/-}$ eggs. (*Left*) Wild-type. (*Middle*) $CD9^{-/-}$. (*Right*) $Tg^{+}CD9^{-/-}$. Right-side of the sets of wild-type and $Tg^{+}CD9^{-/-}$ eggs are enlarged images of the boxed regions. The live eggs were examined, and the internal localization of GM3 in $CD9^{-/-}$ eggs was examined under fixed, permeabilized conditions. (*F*) Comparison of the fluorescent intensities of GM3 stained by antibody in wild-type ($n = 10$), $CD9^{-/-}$ ($n = 9$), and $Tg^{+}CD9^{-/-}$ eggs ($n = 10$) (mean ± SEM). The average values of the wild-type eggs were set to 100%.

$Tg^{+}CD9^{+/-}$ and $CD9^{+/-}$ females (6.0 ± 0.2 and 6.5 ± 0.5) and greater than those from $CD9^{-/-}$ females (0.0 ± 0.0). The $CD9^{+/-}$ females did not exhibit any loss in fertility that could cause a reduction of litter size relative to that of the $CD9^{+/+}$ females (4). Furthermore, the transgene had no effect on normal fertility. These results demonstrate that transgenically expressed CD9-EGFP can compensate for the loss of intrinsic CD9 and yield eggs with the ability to fuse with sperm.

Based on the foregoing evidence, we observed the subcellular localization of CD9-EGFP in "living" $Tg^{+}CD9^{-/-}$ eggs (Fig. 2*A*). As expected, confocal microscopic analysis allowed the visualization of two types of CD9-EGFP localization: intense on the plasma membrane and also in the cytoplasm. Unexpectedly, we found loosely filled, noncompacted CD9-EGFP in the PVS, a space formed between the zona pellucida and the plasma membrane of the egg. The localization of CD9 outside the eggs also was confirmed by Western blot analysis using anti-CD9 mAb (Fig. 2*B*). As shown in the diagram, $CD9^{+/+}$ eggs were mechanically fractionated into denuded eggs and other components (R) using a piezo manipulator (11). The fraction R, containing the zona pellucida and the components in the PVS, was centrifuged and subjected to Western blot analysis. The amount of CD9 in the remnant material from 40 eggs was found to be densitometrically equal to that of 10 zona-free eggs, demonstrating an estimated relative abundance of CD9 in the remnant of 20% per egg. Subsequently, we performed immunoelectron-microscopic analysis on the $CD9^{+/+}$ eggs. We identified the vesicles bound to gold particles inside the PVS (Fig. 2*C*). The sectioned microvilli contained a branched network of actin filaments, whereas the variously sized vesicles (50–250 nm in diameter) had uniformly dense materials rather than actin filaments. We also compared $CD9^{+/+}$, $Tg^{+}CD9^{-/-}$, and $CD9^{-/-}$ eggs by electron-microscopic analysis [supporting information (SI) Fig. S1]. The accumulation of vesicles in the PVS in the $Tg^{+}CD9^{-/-}$ eggs was comparable to that in the $CD9^{+/+}$ eggs, whereas it was not seen in the $CD9^{-/-}$ or germinal vesicle-staged $CD9^{+/+}$ eggs. These results indicate that 20% of the total amount of CD9 is stored as vesicles in the PVS during meiosis.

We next examined the expression of ganglioside GM3, identified as a CD9-associated molecule (12) and a component of exosomes (10), in $CD9^{+/+}$, $CD9^{-/-}$, and $Tg^{+}CD9^{-/-}$ eggs. First, we confirmed the expression of GM3 synthase (ST3GalV/SAT-1) (13) in these eggs by RT-PCR (Fig. 2*D*). Then we investigated the localization of GM3 by immunostaining these live eggs with anti-GM3 mAb (Fig. 2*E*). This antibody has been demonstrated to recognize GM3 in the plasma membrane of cells without treatment for permeabilization (14). Finally, we measured the fluorescent intensities of GM3 in these live eggs (Fig. 2*F*). As expected, in wild-type eggs, GM3 was colocalized with CD9 in the PVS and plasma membrane (Fig. 2*E Left* and Fig. 2*F*). In contrast, in $CD9^{-/-}$ eggs, the fluorescent intensities of GM3 were decreased dramatically in the PVS and plasma membrane (0.4% ± 0.2%, relative to 100% for the $CD9^{+/+}$ eggs), consistent with the loss of CD9 (Fig. 2*E Center* and Fig. 2*F*), whereas GM3 could be detected in the cytoplasm of $CD9^{-/-}$ eggs that had been permeabilized by a detergent after fixation. Moreover, the expression of CD9-EGFP reversed the decrease of GM3 in the PVS and plasma membrane of $CD9^{-/-}$ eggs (25.6 ± 10.7%) (Fig. 2*E Right* and Fig. 2*F*), corresponding to the amount of CD9-EGFP quantified by Western blot analysis (Fig. 1*B*). In addition, electron-microscopic analysis revealed that the number of characteristic membrane structures, termed microvilli (1), were significantly decreased in the $CD9^{-/-}$ eggs compared with the $CD9^{+/+}$ eggs (Fig. S2 *A* and *B*). The numbers of microvilli were increased by ≈50% by the expression of CD9-EGFP in the $CD9^{-/-}$ eggs. The analyses of three types of eggs indicate that CD9- and GM3-containing vesicle release is linked to microvilli formation.

We next investigated the involvement of CD9-containing vesicles in sperm–egg fusion (Fig. 3). We found that, based on the length of microvilli (Fig. S2*C*), zona-intact $Tg^{+}CD9^{-/-}$ eggs can be categorized into two groups (Fig. 3*A*). From single